RC22344 (W0202-055) February 20, 2002
Electrical Engineering

IBM Research Report

The Physical Design of on-Chip Interconnections: Part II: Statistical Model

Mary Y. L. Wisniewski, Emmanuel Yashchin, Robert L. Franch, David Conrady, Giovanni Fiorenza, I. Cevdet Noyan
IBM Research Division
Thomas J. Watson Research Center
P.O. Box 218
Yorktown Heights, NY 10598

Research Division
Almaden - Austin - Beijing - Delhi - Haifa - India - T. J. Watson - Tokyo - Zurich

Abstract

Custom interconnect design complements automated route algorithms which do not guarantee the generation of robust, legal routes for all signals in a ULSI design. Because of the complexity of the route problem in ULSI designs, multiple route solutions are possible, some solutions are more efficient than others, and there is a need for statistical tools to determine whether a designer is following an efficient path. This paper is the second in a series on physical design of on-chip interconnections, and in this paper, we present a statistical framework to quantify the quality of custom interconnections and to optimize physical properties of interconnections in a design. The analytical techniques presented in this series of papers can also be incorporated in semi-custom and ASIC designs and may serve as tools to evaluate and improve various route algorithms.

Keywords

Custom interconnect design, custom interconnection, cumulative effectiveness, netlength effectiveness, via effectiveness.

I. Introduction

An understanding of the role of interconnections in ultra-large-scale-integrated (ULSI) chip design is important to achieve optimal performance in high-speed microprocessors and has implications for the manufacturability and realization of increasingly complex circuits[1], [2], [3], [4], [5], [6], [7], [8], [9], [10], [11], [12]. The use of large numbers of signals in ULSI designs increases design complexity, and the importance of understanding the effects of this increasing complexity has been highlighted by the Semiconductor Industry Association[3]. Moreover, the detailed design of interconnections for these signals also impacts design yield, performance, and power dissipation as well as system cost and information processing ability[4], [13], [14], [15], [16], [17], [18], [19], [20].

Because of the multi-variate nature of the route problem in ULSI designs, a large number of algorithms can be incorporated in the design process. Discriminating among the various algorithms is currently hard since no method to establish efficacy exists.

In this second paper of a series on the physical design of on-chip interconnections, we present a statistical framework to measure the efficacy of a proposed route algorithm before deciding whether to include it in the design process. Here, the real issue addressed is how to decide whether a proposed algorithm actually has a positive impact on the design process, and the goal is to determine whether or not intervention with the algorithm for

select signals is effective in improving the physical properties of these signal routes without adversely affecting physical properties of segments routed with the existing route device, such as an automated router. Decisions regarding the efficacy of such an algorithm can be made based on the statistical considerations presented in this paper. Section II presents a statistical method to quantify interconnection quality and impact of custom interconnections, and Section III describes a method to optimize interconnect physical design. As in[21], this paper also applies the presented techniques to analyze interconnections in the IBM POWER4 Instruction Fetch Unit.

II. Statistical method to quantify interconnection quality and impact of custom interconnections

In this section, we present a method to measure the effectiveness with which unit-level interconnections can be optimized with techniques presented in the first paper of this series.[21] Custom interconnections simply represent one possible pre-route algorithm that can supplement an existing route device, and custom interconnections can be instantiated in the design with designer intervention or with a supplemental computing algorithm.

A. Statistical model of effectiveness

Let R_i denote the area, or region of influence, that physically encloses the new custom interconnections that route ΔN_c^i signals in trial i. $\overline{R_i}$ denotes the complement of R_i, the area in the design that does not contain new custom interconnections, as shown in Fig. 1. In this figure, for trial i, R_i is shaded blue, $\overline{R}_i$ is unshaded, (a) indicates an example of custom interconnections inserted in previous trials, (b) indicates an example of a new custom interconnection in trial i, (c) indicates an example of a route which is routed by an automated router and which partially passes through region R_i, and (d) indicates a signal route generated by the automated router and does not pass through R_i. Let N_c^i denote the total number of signals that have been routed with custom routes in trial i, where $N_c^i = \sum_{j=1}^{i} \Delta N_c^j$.

The total route length $L^{(i)}$ of all signal routes in trial i is composed of four separate components: the total length $\Delta L_c^{(i)}(R_i)$ of new custom interconnections contained in R_i in trial i; the total length $L_c^{(i-1)}$ of all custom routes in previous trials 0 to $i-1$, where $L_c^{(i-1)} =$

$\sum_{j=1}^{i-1} \Delta L_c^{(j)}(R_j)$; the total length $L_o^{(i)}(R_i)$ of route segments routed by an automated router in which at least part of the signal route passes through R_i; and the total length $L_r^{(i)}(\overline{R_i})$ of route segments routed by an automated router in which no part of the signal route passes through R_i, as described by the expression,

$$L^{(i)} = L_c^{(i-1)} + \Delta L_c^{(i)}(R_i) + L_o^{(i)}(R_i) + L_r^{(i)}(\overline{R_i}). \tag{1}$$

The expression for the total number of vias $v^{(i)}$ in all the signal routes in trial i is obtained by substituting v for L in Eqn. 1,

$$v^{(i)} = v_c^{(i-1)} + \Delta v_c^{(i)}(R_i) + v_o^{(i)}(R_i) + v_r^{(i)}(\overline{R_i}), \tag{2}$$

where $v_c^{(i-1)}$ is the total number of vias in all custom interconnections in previous trials 0 to $i-1$, $\Delta v_c^{(i)}(R_i)$ is the total number of vias in new custom interconnections in trial i, $v_o^{(i)}(R_i)$ is the total number of vias in route segments routed by an automated router in which at least part of the signal route passes through R_i, and $v_r^{(i)}(\overline{R_i})$ is the number of vias in route segments routed by an automated router in which no part of the signal route passes through R_i.

To compare the design routes in trial i with design routes in trial $i-1$, we measure the routes in both trials relative to the region of influence R_i of trial i. In this comparison, the total route length of all the signals in trial $i-1$ is described with an expression similar to Eqn. 1,

$$L^{(i-1)} = L_c^{(i-1)} + \Delta L_t^{(i-1)}(R_i) + L_o^{(i-1)}(R_i) + L_r^{(i-1)}(\overline{R_i}), \tag{3}$$

where $\Delta L_t^{(i-1)}(R_i)$ is the total route length in trial $i-1$ of signals targeted to be routed with custom routes in trial i. An expression for the total number of vias in the previous trial $i-1$ is obtained by substituting v for L in Eqn. 3 to obtain the relation,

$$v^{(i-1)} = v_c^{(i-1)} + \Delta v_t^{(i-1)}(R_i) + v_o^{(i-1)}(R_i) + v_r^{(i-1)}(\overline{R_i}), \tag{4}$$

where $\Delta v_t^{(i-1)}(R_i)$ is the total number of vias in trial $i-1$ in signals that are targeted to be routed with custom interconnections in trial i.

In this paper, we will focus most of the discussion on analysis of netlengths of signals in a design; however, an analogous analysis for vias proceeds in a straightforward manner from the analysis of netlengths by substituting v for L throughout the discussion.

Figure 1(a) shows examples of the four types of design routes in trial $i-1$: the custom interconnections (1') that are inserted with length $L_c^{(i-1)}$, the targeted routes (2') in R_i with length $\Delta L_t^{(i-1)}$, routes that partially pass (3') through R_i with length $L_o^{(i-1)}$, and the remaining routes (4') that do not pass through R_i with total length $L_r^{(i-1)}(\overline{R_i})$. Examples of the corresponding design routes in trial i are shown in Fig. 1(b), where the total length of signals represented by those shown in (1)-(4) are represented by the quantities $L_c^{(i-1)}$, $\Delta L_c^{(i)}(R_i)$, $L_o^{(i)}(R_i)$, and $L_r^{(i)}(\overline{R_i})$, respectively. Note that the custom interconnection lengths shown in (1) and (1') are equal to $L_c^{(i-1)}$.

In the following discussion, the simplified notation $\Delta L_c^{(i)}$, $\Delta L_t^{(i-1)}$, $L_o^{(i-1)}$, and $L_r^{(i-1)}$ is employed instead of $\Delta L_c^{(i)}(R_i)$, $\Delta L_t^{(i-1)}(R_i)$, $L_o^{(i-1)}(R_i)$, and $L_r^{(i-1)}(R_i)$, respectively, and full notation is provided only where confusion is possible. We denote $\tilde{L}^{(i-1)} = L^{(i-1)} - L_c^{(i-1)} = \Delta L_t^{(i-1)} + L_o^{(i-1)} + L_r^{(i-1)}$ to represent the length of signals in trial $i-1$ that can potentially be affected in trial i by custom interconnection length $\Delta L_c^{(i)}$ in trial i.

The effectiveness $\epsilon_L^{(i)}$ with which custom interconnections affect the total route length in trial i L^i compared with the total route length in trial $i-1$ is represented by the expression,

$$\epsilon_L^{(i)} = 1 - \frac{L^{(i)} - L_c^{(i-1)}}{\tilde{L}^{(i-1)}}, \tag{5}$$

where the numerator in the second term in Eqn. 5 represents the sum of $\Delta L_c^{(i)}$ and the total route length generated with the automated router. Equation 5 can be expanded in terms of the effectiveness $\epsilon_{L_c}^{(i)}$ of the addition of custom interconnections in R_i, the effectiveness $\epsilon_{L_o}^{(i)}$ of signal segments that are routed by an automated router in which at least part of the signal route passes through R_i, and the effectiveness $\epsilon_{L_r}^{(i)}$ of the remaining route segments that do not pass through R_i, according to the expressions,

$$\epsilon_{L_c}^{(i)} = 1 - \frac{\Delta L_c^{(i)}}{\Delta L_t^{(i-1)}}, \tag{6}$$

$$\epsilon_{L_o}^{(i)} = 1 - \frac{L_o^{(i)}}{L_o^{(i-1)}}, \tag{7}$$

$$\epsilon_{L_r}^{(i)} = 1 - \frac{L_r^{(i)}}{L_r^{(i-1)}}. \tag{8}$$

Substituting Eqns. 6 through 8 into Eqn. 5, we obtain the expression,

$$\epsilon_L^{(i)} = p_{L_t}^{(i-1)} \epsilon_{L_c}^{(i)} + p_{L_o}^{(i-1)} \epsilon_{L_o}^{(i)} + p_{L_r}^{(i-1)} \epsilon_{L_r}^{(i)}, \tag{9}$$

where $p_{L_t}^{(i-1)}$, $p_{L_o}^{(i-1)}$, and $p_{L_t}^{(i-1)}$ are the fraction of $\tilde{L}^{(i-1)}$ targeted for custom interconnections in trial i, the fraction of $\tilde{L}^{(i-1)}$ routed with the automated router in trial i and is connected to route segments that pass through R_i, and the fraction of $\tilde{L}^{(i-1)}$ that does not pass through R_i, respectively, and are given by the expressions,

$$p_{L_t}^{(i-1)} = \frac{\Delta L_t^{(i-1)}}{\tilde{L}^{(i-1)}}, \tag{10}$$

$$p_{L_o}^{(i-1)} = \frac{L_o^{(i-1)}}{\tilde{L}^{(i-1)}}, \tag{11}$$

$$p_{L_r}^{(i-1)} = \frac{L_r^{(i-1)}}{\tilde{L}^{(i-1)}}. \tag{12}$$

We postulate that each of the three effectivenesses given by Eqns. 6 - 8 are independent variables that are distributed according to the normal distribution, according to the expressions:

$$\epsilon_{L_c}^{(i)} \sim N(\mu_{L_c}, \frac{\sigma_{L_c}^2}{\Delta L_t{}^{(i-1)}}) = N(\mu_{L_c}, \sigma_{\epsilon_{L_c}^{(i)}}^2), \tag{13}$$

$$\epsilon_{L_o}^{(i)} \sim N(\mu_{L_o}, \frac{\sigma_{L_o}^2}{L_o{}^{(i-1)}}) = N(\mu_{L_o}, \sigma_{\epsilon_{L_o}^{(i)}}^2), \tag{14}$$

$$\epsilon_{L_r}^{(i)} \sim N(\mu_{L_r}, \frac{\sigma_{L_r}^2}{L_r{}^{(i-1)}}) = N(\mu_{L_r}, \sigma_{\epsilon_{L_r}^{(i)}}^2), \tag{15}$$

where the variables μ_{L_c}, μ_{L_o}, and μ_{L_r} represent the true unknown mean value of each effectiveness, respectively, and the variables $\sigma_{\epsilon_{L_c}^{(i)}}^2$, $\sigma_{\epsilon_{L_o}^{(i)}}^2$, and $\sigma_{\epsilon_{L_r}^{(i)}}^2$ represent the true unknown variance of each effectiveness and are given by the expressions,

$$\sigma_{\epsilon_{L_c}^{(i)}}^2 = \frac{\sigma_{L_c}^2}{\Delta L_t^{(i-1)}}, \tag{16}$$

$$\sigma_{\epsilon_{L_o}^{(i)}}^2 = \frac{\sigma_{L_o}^2}{L_o^{(i-1)}}, \tag{17}$$

$$\sigma_{\epsilon_{L_r}^{(i)}}^2 = \frac{\sigma_{L_r}^2}{L_r^{(i-1)}}. \tag{18}$$

B. Estimation of model parameters

Unbiased estimates of the average value of each effectiveness for n independent trials can be represented by the variables $\hat{\mu}_{L_c}$, $\hat{\mu}_{L_o}$, and $\hat{\mu}_{L_r}$, respectively, which can be obtained

from a calculation of the weighted average of the appropriate effectiveness over n trials according to the following expressions,

$$\hat{\mu}_{L_c} = \frac{\sum_{i=1}^{n} \epsilon_{L_c}^{(i)} \Delta L_t^{(i-1)}}{\sum_{j=1}^{n} \Delta L_t^{(j-1)}}, \tag{19}$$

$$\hat{\mu}_{L_o} = \frac{\sum_{i=1}^{n} \epsilon_{L_o}^{(i)} L_o^{(i-1)}}{\sum_{j=1}^{n} L_o^{(j-1)}}, \tag{20}$$

$$\hat{\mu}_{L_r} = \frac{\sum_{i=1}^{n} \epsilon_{L_r}^{(i)} L_r^{(i-1)}}{\sum_{j=1}^{n} L_r^{(j-1)}}. \tag{21}$$

Each of the means $\hat{\mu}_{L_c}$, $\hat{\mu}_{L_o}$, and $\hat{\mu}_{L_r}$, has corresponding variance $Var(\hat{\mu}_{L_c})$, $Var(\hat{\mu}_{L_o})$, and $Var(\hat{\mu}_{L_r})$, respectively. The three variances can be represented by the variables $Var(\hat{\mu}_{L_c}) = \sigma^2(\hat{\mu}_{L_c})$, $Var(\hat{\mu}_{L_o}) = \sigma^2(\hat{\mu}_{L_o})$, and $Var(\hat{\mu}_{L_r}) = \sigma^2(\hat{\mu}_{L_r})$, which are obtained with the expressions,

$$\sigma^2(\hat{\mu}_{L_c}) = \langle (\hat{\mu}_{L_c} - \mu_{L_c})^2 \rangle = \frac{\sum_{j=1}^{n} \langle (\epsilon_{L_c}^{(j)} - \mu_{L_c})^2 \rangle (\Delta L_t^{(j-1)})^2}{(\sum_{j=1}^{n} \Delta L_t^{(j-1)})^2} = \frac{\sigma_{L_c}^2}{\sum_{j=1}^{n} \Delta L_t{}^{(j-1)}}, \tag{22}$$

$$\sigma^2(\hat{\mu}_{L_o}) = \langle (\hat{\mu}_{L_o} - \mu_{L_o})^2 \rangle = \frac{\sum_{j=1}^{n} \langle (\epsilon_{L_o}^{(j)} - \mu_{L_o})^2 \rangle (L_o^{(j-1)})^2}{(\sum_{j=1}^{n} L_o^{(j-1)})^2} = \frac{\sigma_{L_o}^2}{\sum_{j=1}^{n} L_o{}^{(j-1)}}, \tag{23}$$

$$\sigma^2(\hat{\mu}_{L_r}) = \langle (\hat{\mu}_{L_r} - \mu_{L_r})^2 \rangle = \frac{\sum_{j=1}^{n} \langle \epsilon_{L_r}^{(j)} - \mu_{L_r} \rangle^2 (L_r^{(j-1)})^2}{(\sum_{j=1}^{n} L_r^{(j-1)})^2} = \frac{\sigma_{L_r}^2}{\sum_{j=1}^{n} L_r{}^{(j-1)}}, \tag{24}$$

with Eqns. 13 - 18.

In this formulation, the normalized means $\frac{\hat{\mu}_{L_c} - \mu_{L_c}}{\sigma(\hat{\mu}_{L_c})}$, $\frac{\hat{\mu}_{L_o} - \mu_{L_o}}{\sigma(\hat{\mu}_{L_o})}$, and $\frac{\hat{\mu}_{L_r} - \mu_{L_r}}{\sigma(\hat{\mu}_{L_r})}$ are distributed according to the normal distribution with zero mean and unity variance, as shown by the expressions,

$$\frac{\hat{\mu}_{L_c} - \mu_{L_c}}{\sigma(\hat{\mu}_{L_c})} \sim N(0,1), \tag{25}$$

$$\frac{\hat{\mu}_{L_o} - \mu_{L_o}}{\sigma(\hat{\mu}_{L_o})} \sim N(0,1), \tag{26}$$

$$\frac{\hat{\mu}_{L_r} - \mu_{L_r}}{\sigma(\hat{\mu}_{L_r})} \sim N(0,1). \tag{27}$$

The notation $\sigma(\hat{\mu})$ and $\sigma^2(\hat{\mu})$ represents the standard deviation and variance, respectively, of the estimator $\hat{\mu}$, as shown in Eqns. 22 - 24 above. Furthermore, the standard error of $\hat{\mu}$ will be denoted by $\hat{\sigma}(\hat{\mu})$, which is obtained by substituting $\hat{\sigma}^2$ for σ^2 into the

formula for $\sigma(\hat{\mu})$. For example, substituting $\hat{\sigma}^2_{L_c}$, $\hat{\sigma}^2_{L_o}$, and $\hat{\sigma}^2_{L_r}$ for $\sigma^2_{L_c}$, $\sigma^2_{L_o}$, and $\sigma^2_{L_r}$, respectively, in Eqns. 22 - 24, and taking the square root of both sides of the equations, we obtain the following expressions for the standard error of the three unbiased estimates $\hat{\mu}_{L_c}$, $\hat{\mu}_{L_o}$, and $\hat{\mu}_{L_r}$ of the effectivenesses,

$$\hat{\sigma}(\hat{\mu}_{L_c}) = \frac{\hat{\sigma}_{L_c}}{\sqrt{\sum_{j=1}^{n} \Delta L_t^{(j-1)}}}, \tag{28}$$

$$\hat{\sigma}(\hat{\mu}_{L_o}) = \frac{\hat{\sigma}_{L_o}}{\sqrt{\sum_{j=1}^{n} L_o^{(j-1)}}}, \tag{29}$$

$$\hat{\sigma}(\hat{\mu}_{L_r}) = \frac{\hat{\sigma}_{L_r}}{\sqrt{\sum_{j=1}^{n} L_r^{(j-1)}}}, \tag{30}$$

respectively.

In each trial i, the measured route lengths of the custom routes, other routes, and the rest of the routes provide unbiased estimates of $\sigma^2_{L_c}$, $\sigma^2_{L_o}$, and $\sigma^2_{L_r}$, respectively, from the relations,

$$\langle (\epsilon^{(i)}_{L_c} - \hat{\mu}_{L_c})^2 \rangle = \sigma^2_{L_c} \left(\frac{1}{\tilde{v}^{(i-1)}_{L_t}} \right), \tag{31}$$

$$\langle (\epsilon^{(i)}_{L_o} - \hat{\mu}_{L_o})^2 \rangle = \sigma^2_{L_o} \left(\frac{1}{\tilde{v}^{(i-1)}_{L_o}} \right), \tag{32}$$

$$\langle (\epsilon^{(i)}_{L_r} - \hat{\mu}_{L_r})^2 \rangle = \sigma^2_{L_r} \left(\frac{1}{\tilde{v}^{(i-1)}_{L_r}} \right), \tag{33}$$

where the quantities $\tilde{v}^{(i-1)}_{L_t}$, $\tilde{v}^{(i-1)}_{L_o}$, and $\tilde{v}^{(i-1)}_{L_r}$ are given by the expressions,

$$\tilde{v}^{(i-1)}_{L_t} = \left(\frac{1}{\Delta L_t^{(i-1)}} - \frac{1}{\sum_{j=1}^{n} \Delta L_t^{(j-1)}} \right)^{-1}, \tag{34}$$

$$\tilde{v}^{(i-1)}_{L_o} = \left(\frac{1}{L_o^{(i-1)}} - \frac{1}{\sum_{j=1}^{n} L_o^{(j-1)}} \right)^{-1}, \tag{35}$$

$$\tilde{v}^{(i-1)}_{L_r} = \left(\frac{1}{L_r^{(i-1)}} - \frac{1}{\sum_{j=1}^{n} L_r^{(j-1)}} \right)^{-1}. \tag{36}$$

The derivation of the right-hand side of Eqn. 31 begins with the expansion of the left-hand side of this equation to obtain the expression,

$$\begin{aligned}\langle(\epsilon_{L_c}^{(i)} - \hat{\mu}_{L_c})^2\rangle &= \langle(\epsilon_{L_c}^{(i)} - \frac{\sum_{j=1}^{n} \Delta L_t^{(j-1)} \epsilon_{L_c}^{(j)}}{\sum_{j=1}^{n} \Delta L_t^{(j-1)}})^2\rangle \\ &= \langle(\epsilon_{L_c}^{(i)} - \mu_{L_c} - \frac{\sum_{j=1}^{n} \Delta L_t^{(j-1)} (\epsilon_{L_c}^{(j)} - \mu_{L_c})}{\sum_{j=1}^{n} \Delta L_t^{(j-1)}})^2\rangle \end{aligned} \quad (37)$$

Next, the terms on the right-hand side of Eqn. 37 are expanded and then combined with a common denominator, as shown in the derivation below,

$$\begin{aligned}\langle(\epsilon_{L_c}^{(i)} - \hat{\mu}_{L_c})^2\rangle &= \frac{\langle(\sum_{j\neq i}(\epsilon_{L_c}^{(i)} - \mu_{L_c})\Delta L_t^{(j-1)} - \sum_{j\neq i} \Delta L_t^{(j-1)}(\epsilon_{L_c}^{(j)} - \mu_{L_c}))^2\rangle}{(\sum_{i=1}^{n} \Delta L_t^{(i-1)})^2} \\ &= \frac{\langle(\sum_{j\neq i} \Delta L_t^{(j-1)})^2(\epsilon_{L_c}^{(i)} - \mu_{L_c})^2\rangle + \langle(\sum_{j\neq i} \Delta L_t^{(j-1)}[\epsilon_{L_c}^{(j)} - \mu_{L_c}])^2\rangle}{(\sum_{i=1}^{n} \Delta L_t^{(i-1)})^2} \\ &= \frac{(\sum_{j\neq i} \Delta L_t^{(j-1)})^2 \frac{\sigma_{L_c}^2}{\Delta L_t^{(i-1)}} + \sum_{j\neq i}(\Delta L_t^{(j-1)})^2 \frac{\sigma_{L_c}^2}{\Delta L_t^{(j-1)}}}{(\sum_{i=1}^{n} \Delta L_t^{(i-1)})^2} \\ &= \frac{(\sum_{j=1}^{n} \Delta L_t^{(j-1)} - \Delta L_t^{(i-1)})^2 \frac{\sigma_{L_c}^2}{\Delta L_t^{(i-1)}} + (\sum_{j=1}^{n} \Delta L_t^{(j-1)} - \Delta L_t^{(i-1)})\sigma_{L_c}^2}{(\sum_{i=1}^{n} \Delta L_t^{(i-1)})^2} \\ &= \frac{(\sum_{j=1}^{n} \Delta L_t^{(j-1)} - \Delta L_t^{(i-1)})\sigma_{L_c}^2}{(\sum_{i=1}^{n} \Delta L_t^{(i-1)})^2}(\frac{\sum_{j=1}^{n} \Delta L_t^{(j-1)} - \Delta L_t^{(i-1)}}{\Delta L_t^{(i-1)}} + 1) \\ &= \frac{(\sum_{j=1}^{n} \Delta L_t^{(j-1)} - \Delta L_t^{(i-1)})\sigma_{L_c}^2}{(\sum_{i=1}^{n} \Delta L_t^{(i-1)})^2} \frac{\sum_{j=1}^{n} \Delta L_t^{(j-1)}}{\Delta L_t^{(i-1)}} \\ &= \sigma_{L_c}^2 \left(\frac{1}{\tilde{v}_{L_t}^{(i-1)}}\right), \end{aligned} \quad (38)$$

which is Eqn. 31. The derivations of Eqns. 32 and 33 proceed in a similar manner. Therefore, setting Eqn. 31 and the last line of Eqn. 38 equal, $\langle(\epsilon_{L_c}^{(i)} - \hat{\mu}_{L_c})^2\rangle \cdot \tilde{v}_{L_t}^{(i-1)}$ can be viewed as an unbiased estimate of $\sigma_{L_c}^2$ based exclusively on results of the i^{th} trial. Similarly, the results of the i^{th} trial provide unbiased estimates $\langle(\epsilon_{L_o}^{(i)} - \hat{\mu}_{L_o})^2\rangle \cdot \tilde{v}_{L_o}^{(i-1)}$ and $\langle(\epsilon_{L_r}^{(i)} - \hat{\mu}_{L_r})^2\rangle \cdot \tilde{v}_{L_r}^{(i-1)}$ of $\sigma_{L_o}^2$ and $\sigma_{L_r}^2$, respectively.

Unbiased estimates of $\sigma_{L_c}^2$, $\sigma_{L_o}^2$, and $\sigma_{L_r}^2$ based on the set of n trials can be represented by the variables $\hat{\sigma}_{L_c}^2$, $\hat{\sigma}_{L_o}^2$, and $\hat{\sigma}_{L_r}^2$, respectively, which can be obtained by calculating the

average of the observed deviations of the data over n trials and are given by the relations,

$$\hat{\sigma}^2_{L_c} = \frac{1}{n}\sum_{i=1}^{n}(\epsilon^{(i)}_{L_c} - \hat{\mu}_{L_c})^2 \cdot \tilde{v}^{(i-1)}_{L_t} = \frac{1}{n}\sum_{i=1}^{n}(B^{(i)}_{L_c})^2, \tag{39}$$

$$\hat{\sigma}^2_{L_o} = \frac{1}{n}\sum_{i=1}^{n}(\epsilon^{(i)}_{L_o} - \hat{\mu}_{L_o})^2 \cdot \tilde{v}^{(i-1)}_{L_o} = \frac{1}{n}\sum_{i=1}^{n}(B^{(i)}_{L_o})^2, \tag{40}$$

$$\hat{\sigma}^2_{L_r} = \frac{1}{n}\sum_{i=1}^{n}(\epsilon^{(i)}_{L_r} - \hat{\mu}_{L_r})^2 \cdot \tilde{v}^{(i-1)}_{L_r} = \frac{1}{n}\sum_{i=1}^{n}(B^{(i)}_{L_r})^2, \tag{41}$$

where the quantities $B^{(i)}_{L_c}$, $B^{(i)}_{L_o}$, and $B^{(i)}_{L_r}$ represent the normalized means in each trial i and are given by the expressions,

$$B^{(i)}_{L_c} = (\epsilon^{(i)}_{L_c} - \hat{\mu}_{L_c}) \cdot \sqrt{\tilde{v}^{(i-1)}_{L_t}}, \tag{42}$$

$$B^{(i)}_{L_o} = (\epsilon^{(i)}_{L_o} - \hat{\mu}_{L_o}) \cdot \sqrt{\tilde{v}^{(i-1)}_{L_o}}, \tag{43}$$

$$B^{(i)}_{L_r} = (\epsilon^{(i)}_{L_r} - \hat{\mu}_{L_r}) \cdot \sqrt{\tilde{v}^{(i-1)}_{L_r}}. \tag{44}$$

The normalized means $\{B^{(i)}_{L_c}\}$, $\{B^{(i)}_{L_o}\}$, and $\{B^{(i)}_{L_r}\}$ are distributed according to the normal distribution with zero mean and variance $\sigma^2_{L_c}$, $\sigma^2_{L_o}$, and $\sigma^2_{L_r}$, respectively, as described by the expressions,

$$\{B^{(i)}_{L_c}\} \sim N(0, \sigma^2_{L_c}), \tag{45}$$

$$\{B^{(i)}_{L_o}\} \sim N(0, \sigma^2_{L_o}), \tag{46}$$

$$\{B^{(i)}_{L_r}\} \sim N(0, \sigma^2_{L_r}). \tag{47}$$

Scatterplots of the *B-values* (e.g., $\{B^{(i)}_{L_c}\}$ as a function of $\{B^{(i)}_{L_o}\}$) assist in an assessment of the independence of the three types of routes: custom interconnections, other routes that pass through R_i, and the rest of routes that do not pass through R_i.

When the standard errors $\hat{\sigma}_{L_c}$, $\hat{\sigma}_{L_o}$, and $\hat{\sigma}_{L_r}$ are substituted for the unknown quantities σ_{L_c}, σ_{L_o}, and σ_{L_r} in Eqns. 25, 26 and 27, respectively, the three ratios $\frac{\hat{\mu}_{L_c}-\mu_{L_c}}{\hat{\sigma}(\hat{\mu}_{L_c})}$, $\frac{\hat{\mu}_{L_o}-\mu_{L_o}}{\hat{\sigma}(\hat{\mu}_{L_o})}$, and $\frac{\hat{\mu}_{L_r}-\mu_{L_r}}{\hat{\sigma}(\hat{\mu}_{L_r})}$ are no longer distributed according to the normal distribution $N(0,1)$. Instead, these ratios can be approximated by the T_{n-1} distribution, a *t (Student)* random variable with $n-1$ degrees of freedom. The T_{n-1} distribution enables the construction of *p-values* that assess the extent to which the data contradicts the hypothesis that an effect is zero (for example, the hypothesis that $\mu_{L_c} = 0$; the hypothesis that $\mu_{L_o} = 0$; or

the hypothesis that $\mu_{L_r} = 0$); it could also obtain confidence bounds for the effect. The *p-value* for μ_{L_c} can be represented by the variable *p-value*(μ_{L_c}) and is the probability that the value of the estimator $\hat{\mu}_{L_c}$ is more extreme than the observed value of the mean, $\tilde{\mu}_{L_c}$, based on n trials[22]. In the case of custom interconnections, we postulate *a priori* that the effect is greater than zero; therefore, only the lower confidence bound is computed, and the *p-value* is given by the expression,

$$\begin{aligned} p-value(\mu_{L_c}) &= Pr\{\hat{\mu}_{L_c} > \tilde{\mu}_{L_c} | \mu_{L_c} = 0\} \\ &= Pr\{\frac{\hat{\mu}_{L_c} - 0}{\hat{\sigma}(\hat{\mu}_{L_c})} > \frac{\tilde{\mu}_{L_c} - 0}{\hat{\sigma}(\hat{\mu}_{L_c})} | \mu_{L_c} = 0\} \\ &= Pr\{T_{n-1} > \frac{\tilde{\mu}_{L_c}}{\hat{\sigma}(\hat{\mu}_{L_c})}\}. \end{aligned} \tag{48}$$

In a similar manner, the *p-values* for μ_{L_o} and μ_{L_r} can be represented by the variables *p-value*(μ_{L_o}) and *p-value*(μ_{L_r}), respectively. In the case of the other routes that pass through R_i, we do not make an *a priori* directional statement; therefore, two-sided confidence intervals are computed and the strength of evidence against the hypothesis of zero effect is measured based on the *p-value*(μ_{L_o}) given by the expression,

$$\begin{aligned} p-value(\mu_{L_o}) &= Pr\{\mid T_{n-1} \mid > \mid \frac{\tilde{\mu}_{L_o}}{\hat{\sigma}(\hat{\mu}_{L_o})} \mid\} \\ &= 2 \cdot Pr\{T_{n-1} > \mid \frac{\tilde{\mu}_{L_o}}{\hat{\sigma}(\hat{\mu}_{L_o})} \mid\}. \end{aligned} \tag{49}$$

Similarly, in the case of the rest of the routes that do not pass through R_i, we also do not make an *a priori* directional statement; a two-sided confidence interval is also computed in this case, and the *p-value*(μ_{L_r}) is given by the expression,

$$\begin{aligned} p-value(\mu_{L_r}) &= Pr\{\mid T_{n-1} \mid > \mid \frac{\tilde{\mu}_{L_r}}{\hat{\sigma}(\hat{\mu}_{L_r})} \mid\} \\ &= 2 \cdot Pr\{T_{n-1} > \mid \frac{\tilde{\mu}_{L_r}}{\hat{\sigma}(\hat{\mu}_{L_r})} \mid\}. \end{aligned} \tag{50}$$

Now we will discuss how to compute the confidence bounds for the unknown means μ_{L_c}, μ_{L_o}, and μ_{L_r}. The 95% Lower Confidence Bound (LCB) for μ_{L_c} can be represented by the variable $LCB_{0.95,\mu_{L_c}}$. This quantity is obtained with the same relationship as above. Since

$$Pr\{\frac{\hat{\mu}_{L_c} - \mu_{L_c}}{\hat{\sigma}(\hat{\mu}_{L_c})} \leq t_{n-1,0.95}\} = 0.95, \tag{51}$$

it follows that $LCB_{0.95,\mu_{L_c}}$ is given by the expression,

$$LCB_{0.95,\mu_{L_c}} = \hat{\mu}_{L_c} - t_{n-1,0.95} \cdot \hat{\sigma}(\hat{\mu}_{L_c}) = \hat{\mu}_{L_c} - t_{n-1,0.95} \cdot \frac{\hat{\sigma}_{L_c}}{\sqrt{\sum_{j=1}^{n} \Delta L_t^{(j-1)}}}. \quad (52)$$

The two-sided 95% confidence intervals for μ_{L_o} are given by a pair of bounds $[LCB_{0.975,\mu_{L_o}}$, $UCB_{0.975,\mu_{L_o}}]$ given by the relations,

$$[LCB_{0.975,\mu_{L_o}}, UCB_{0.975,\mu_{L_o}}] = \hat{\mu}_{L_o} \pm t_{n-1,0.975} \cdot \hat{\sigma}(\hat{\mu}_{L_o}). \quad (53)$$

The two-sided interval for μ_{L_r} is obtained analogously.

B.1 Application to the POWER4 DD1 IFU

We apply the preceding analysis to quantify the physical properties of interconnections in the Instruction Fetch Unit (IFU) of the IBM POWER4 microprocessor[25], [26], [27], [28]. The IFU is routed six times (n=6) to generate six *trials*; each *trial* has a different value of N_c and region of influence R_i. Each trial contains an additional number of custom interconnections $\Delta N_c^{(i)}$ compared to the number in the previous trial. Figure 2 shows a schematic of Fig. 1 applied to the case of the IFU. Each trial i has a corresponding different region of influence R_i indicated by the shaded regions in Fig. 3. Equations 5 - 8 and 10 - 12 determine the values for the netlength effectivenesses $\epsilon_{L_c}^{(i)}$, $\epsilon_{L_o}^{(i)}$, $\epsilon_{L_r}^{(i)}$, $\epsilon_L^{(i)}$ and netlength fractions $p_{L_t}^{(i-1)}$, $p_{L_o}^{(i-1)}$, $p_{L_r}^{(i-1)}$ for each trial i that are shown in Table I. Similar equations for vias determine the values for the via effectivenesses $\epsilon_{v_c}^{(i)}$, $\epsilon_{v_o}^{(i)}$, $\epsilon_{v_r}^{(i)}$, $\epsilon_v^{(i)}$, and via fractions $p_{v_t}^{(i-1)}$, $p_{v_o}^{(i-1)}$, $p_{v_r}^{(i-1)}$, that are shown in Table I. These two tables also show the corresponding values for the netlengths $\Delta L_t^{(i-1)}$, $L_o^{(i-1)}$, $L_r^{(i-1)}$, $L^{(i-1)}$ and vias $\Delta v_t^{(i-1)}$, $v_o^{(i-1)}$, $v_r^{(i-1)}$, and $v^{(i-1)}$.

Scatterplots of the *B-values* for interconnect netlengths and vias provide a graphical assessment of the degree of independence of the three types of routes: custom interconnections, other routes that pass through R_i, and the rest of the routes that do not pass through R_i. Scatterplots for the DD1 IFU are shown in Figures 4 and 5. These plots show *B-values* for netlengths $\{B_{L_c}^{(i)}\}$, $\{B_{L_o}^{(i)}\}$, $\{B_{L_r}^{(i)}\}$ and *B-values* for vias $\{B_{v_c}^{(i)}\}$, $\{B_{v_o}^{(i)}\}$, $\{B_{v_r}^{(i)}\}$, respectively, obtained with Eqns. 34 - 36 and Eqns. 42 - 44 for each of the $n = 6$ trials.

Table II shows a summary of the results for netlengths and vias for all $n = 6$ trials in the DD1 IFU. The table shows values of the *mean*, *standard error*, *p-value*, 95% *LCB* for

custom interconnections and 95% confidence intervals for other routes that pass through R_i and for the rest of the routes that do not pass through R_i. The values are obtained with Eqns. 19 - 21, 22 - 24, 48 - 49, and 52 - 53, respectively. The table shows that the estimated effect of custom interconnect intervention is distinctly positive and that the intervention reduces the total netlength by about 6.7%. The effect is statistically significant; the associated $p\text{-}value(\mu_{L_c}) = 0.015$; the 95% LCB for this effect is $6.7\% - 2.015(2.3\%) = 2.2\% > 0$. For other routes that pass through R_i, we obtain $p\text{-}value(\mu_{L_o}) = 0.039 < 0.05$, which indicates evidence that routes in the domain of influence are negatively affected by the intervention with custom interconnections. The magnitude of this impact can be characterized by the confidence interval for μ_{L_o} obtained with Eqn. 53: $-2.36\% \pm 2.57(0.8\%) = -2.36\% \pm 2.18\% = [-4.5\%, -0.2\%]$. For the rest of the routes that do not pass through R_i, however, we have no evidence of negative impact caused by the custom routing activity: the effect is $\tilde{\mu}_{L_r} = -0.07\%$ with standard error 0.091%, resulting in $p\text{-}value(\mu_{L_r}) = 0.46$; the 95% confidence interval for μ_{L_r} is $-0.07\% \pm 2.57(0.09\%) = -0.07\% \pm 0.23\% \sim [-0.31\%, 0.2\%]$. Any degradation of the netlengths of non-custom interconnections can be addressed by determining if these routes are timing-critical signals or have extremely poor routes; if so, custom interconnections can be applied for these signals in a subsequent trial.

For the case of vias, Table II indicates that intervention with custom interconnections has a strong positive effect on the number of vias in custom routes in R_i. For example, the number of vias is reduced by approximately 65.4%; this effect is statistically significant as the associated $p\text{-}value(\mu_{v_c}) = 0.000013$; the 95% LCB is $65.4\% - 2.015(4.4\%) = 56.5\% >> 0$. For the other routes and the rest of the routes, there is no evidence of negative impact caused by the custom routing activity. For the other routes, the effect is $\tilde{\mu}_{v_o} = -4.1\%$ with standard error 2.2%, resulting in $p\text{-}value(\mu_{v_o}) = 0.12 > 0.05$; the 95% confidence interval for μ_{v_o} is $-4.1\% \pm 2.57(2.2\%) \sim [-9.7\%, 1.5\%]$. For the rest of the routes, the estimated effect is $\tilde{\mu}_{v_r} = 0.085\%$ with standard error 0.43%, resulting in $p\text{-}value(\mu_{v_r}) = 0.85 > 0.05$; the 95% confidence interval for μ_{v_r} is $0.085\% \pm 2.57(0.43\%) \sim [-1.0\%, 1.2\%]$.

B.2 Application to the POWER4 DD2 IFU (reduced-area design)

The statistical analysis can also be applied to quantify the physical properties of interconnections in a reduced-area DD2 IFU. The DD2 IFU is also routed six times (n=6); each of the six *trials* has a different value of N_c^i. Figure 10 shows the region of influence R_i in each of the six trials i as the shaded region indicated. Table XIII shows values for the effectivenesses for netlengths $\epsilon_{Lc}^{(i)}$, $\epsilon_{Lo}^{(i)}$, $\epsilon_{Lr}^{(i)}$, $\epsilon_{L}^{(i)}$ and netlength fractions $p_{Lt}^{(i-1)}$, $p_{Lo}^{(i-1)}$, $p_{Lr}^{(i-1)}$ for each trial i as well as values for effectivenesses for vias $\epsilon_{vc}^{(i)}$, $\epsilon_{vo}^{(i)}$, $\epsilon_{vr}^{(i)}$, $\epsilon_{v}^{(i)}$ and via fractions $p_{vt}^{(i-1)}$, $p_{vo}^{(i-1)}$, $p_{vr}^{(i-1)}$.

Scatterplots of the *B-values* for the DD2 IFU are shown in Figures 11 and 12. As for the DD1 IFU, these plots show *B-values* for netlengths $\{B_{Lc}^{(i)}\}$, $\{B_{Lo}^{(i)}\}$, $\{B_{Lr}^{(i)}\}$ and *B-values* for vias $\{B_{vc}^{(i)}\}$, $\{B_{vo}^{(i)}\}$, $\{B_{vr}^{(i)}\}$, respectively, obtained with Eqns. 34- 36 and Eqns. 42- 44 for each trial in the DD2 IFU.

A summary of the results for netlengths and vias for all $n = 6$ trials in the DD2 IFU is shown in Table XIV. Note that the DD2 results are uniformly consistent with the DD1 results. As for the DD1 IFU, the table shows that the estimated effect of custom interconnections in the DD2 IFU is distinctly positive, reducing the total netlength by about 10.3%. This effect is statistically significant as the associated *p-value*$(\mu_{Lc}) = 0.00051$; the 95% *LCB* for this effect is $10.3\% - 2.015(1.5\%) = 7.3\% > 0$. For other routes that pass through R_i, the *p-value*$(\mu_{Lo}) = 0.042 < 0.05$, which indicates evidence that routes in R_i are negatively affected by the custom route activity. The magnitude of this impact can be characterized by the confidence interval for μ_{Lo} obtained via Eqn. 53: $-2.9\% \pm 2.57(1.1\%) = -2.9\% \pm 2.83\% = [-5.6\%, -0.15\%]$. These signals tend to be control signals that cross R_i; these signals are not timing-critical in contrast with routes for the dataflow signals (buses) that are timing-critical and for which custom interconnections are inserted. Therefore, even though netlengths of control signal routes are increased slightly as the custom interconnections are added in the design, the routes of these controls signals still meet the design timing and electrical requirements (that is, these signals meet the design timing requirements and are free of violations and do not contain design-rule errors). For the rest of the routes that do not pass through R_i, however, there is no evidence of negative impact caused by the custom routing activity; the estimated effect

is $\tilde{\mu}_{L_r} = 0.044\%$ with standard error 0.05%, resulting in $p\text{-}value(\mu_{L_r}) = 0.41$. The 95% confidence interval for μ_{L_r} is $0.044\% \pm 2.57(0.05\%) = 0.044\% \pm 0.13\% \sim [-0.17\%, 0.084\%]$. Any degradation of the netlengths of non-custom routes can be addressed by determining if these signals are timing-critical signals or if the routes are extremely poor; if so, custom interconnections can route these signals in a subsequent trial.

For vias, Table XIV indicates that intervention with custom interconnections has a strong positive effect on the number of vias in custom interconnections in R_i. For example, the number of vias is reduced by about 63.7%; this effect is statistically significant as the associated $p\text{-}value(\mu_{v_c}) = 0.000015$; the 95% LCB is $63.7\% - 2.015(4.5\%) = 54.7\% >> 0$. Furthermore, for the other routes and the rest of the routes, there is no evidence of negative impact caused by the custom routing activity. For the other routes, the estimated effect is $\tilde{\mu}_{v_o} = -3.7\%$ with standard error 2.4%, resulting in $p\text{-}value(\mu_{v_o}) = 0.195 > 0.05$; the 95% confidence interval for μ_{v_o} is $-3.7\% \pm 2.57(2.4\%) \sim [-9.9\%, 2.6\%]$. For the rest of the routes, the estimated effect is $\tilde{\mu}_{v_r} = 0.36\%$ with standard error 0.57%, resulting in $p\text{-}value(\mu_{v_r}) = 0.55 > 0.05$; the 95% confidence interval for μ_{v_r} is $0.36\% \pm 2.57(0.57\%) \sim [-1.1\%, 1.8\%]$.

C. Cumulative effectiveness

The cumulative effectiveness of netlengths and vias in a given trial i compared with trial 0 can be expressed according to the following relations,

$$\epsilon_L^{(i)(0)} = 1 - \frac{L^{(i)} - L_c^{(0)}(R_{i,0})}{L^{(0)} - L_c^{(0)}(R_{i,0})}, \tag{54}$$

and

$$\epsilon_v^{(i)(0)} = 1 - \frac{v^{(i)} - v_c^{(0)}(R_{i,0})}{v^{(0)} - v_c^{(0)}(R_{i,0})}, \tag{55}$$

where $\epsilon_L^{(i)(0)}$ denotes the netlength cumulative effectiveness for signal routes in trial i compared with trial 0, and $\epsilon_v^{(i)(0)}$ denotes the via cumulative effectiveness for signal routes in trial i compared with trial 0. The notation $\epsilon_L^{(i)(0)}$ and $\epsilon_v^{(i)(0)}$ indicates that the effectiveness in trial i is to be calculated relative to the original data for netlengths and vias, respectively, obtained in trial 0. Similarly, the notation $R_{i,0}$ indicates that for these calculations, the region of influence consists of the entire area that encloses custom interconnections

for all N_c^i signals that have been added in the design in *trial 1* through *trial i*. Since the 0^{th} trial contains no custom routes, $L_c^{(0)}(R_{i,0}) = 0$, $L_c^{(0)}(R_{i,0}) = 0$, $v_c^{(0)}(R_{i,0}) = 0$, and $v_c^{(0)}(R_{i,0}) = 0$, and Eqns. 54 and 55 reduce to the expressions,

$$\epsilon_L^{(i)(0)} = 1 - \frac{L^{(i)}}{L^{(0)}}, \tag{56}$$

and

$$\epsilon_v^{(i)(0)} = 1 - \frac{v^{(i)}}{v^{(0)}}, \tag{57}$$

respectively, for each trial $i \leq n$.

The cumulative effectiveness is directly related to effectivenesses observed in the individual steps, namely,

$$\epsilon_L^{(i)(0)} = \epsilon_L^{(1)} + (\frac{L^{(1)} - L_c^{(1)}}{L_o})\epsilon_L^{(2)} + ... + (\frac{L^{(i-1)} - L_c^{(i-1)}}{L_o})\epsilon_L^{(i)}. \tag{58}$$

C.1 Application to the POWER4 DD1 IFU

Figures 6(a) and 6(b) show the cumulative effectivenesses for netlengths $\epsilon_L^{(i)(0)}$ and vias $\epsilon_v^{(i)(0)}$, respectively, for trials $i \leq n = 6$. The figure shows that the projected cumulative effectiveness for both netlengths and vias tends to increase with each additional trial i. The figure shows that the cumulative effectivenesses for netlengths and vias are 0.41% and 19.3%, respectively, for trial $i = n = 6$.

C.2 Application to the POWER4 DD2 IFU

The behavior of the DD2 IFU cumulative effectiveness is similar to that exhibited for the DD1 IFU. Figures 13(a) and 13(b) show the cumulative effectivenesses for netlengths $\epsilon_L^{(i)(0)}$ and vias $\epsilon_v^{(i)(0)}$, respectively, for trials $i \leq n = 6$. As in the DD1 IFU, the projected cumulative effectiveness for both netlengths and vias tends to increase with each additional trial i. The figure shows that the cumulative effectivenesses for netlengths and vias are 1.45% and 20.7%, respectively, after trial $n = 6$. These values are consistent with those observed for the DD1 IFU.

III. Method to optimize interconnect physical design

In Section II, we presented methods for design improvement based on the combined effort of an automated router and an algorithm for custom interconnect design. In practice, the

operation of automated routers is governed by parameters such as via costs or route costs for horizontal wires and vertical wires.

In custom design, once the set of interconnections in a design is error-free and satisfies all design requirements, further iterations can be performed to minimize total netlength and total number of vias, minimize cost, and optimize design performance and yield. Currently there is no good method for designers to optimize physical characteristics of design interconnections to achieve these goals.

In this section, we discuss the selection of automated router parameters to achieve improvement in interconnect physical characteristics. Choice of these parameters will generally not negate the positive impact obtained with custom interconnect intervention because the custom interconnect activity focuses on complex route problems that the automated router is unable to address. There are several ways to select automatic router parameters to optimize interconnect physical characteristics; for example, one could use Experimental Design techniques, such as the Simplex Method or Response Surface Method[23]. In this paper, we choose a simple exploration method; the *optimized design* obtained in the course of its use is associated with non-trivial improvement; we will not make claims regarding its optimality in the strict mathematical sense.

Also in this section, we present a statistical-based decision framework for physical design that facilitates decisions to optimize total netlength and total via number. As such, this framework provides designers with quantitative metrics of their efforts.

A. Impact of reduction in design area

It is desirable to reduce design area, where possible, in order to increase the number of manufacturable chips per wafer. We measure the effect of custom interconnect intervention on CPU runtime required by the automated router to complete routes for the remaining signals. Next, we quantify the proportion of upper-level metal in short routes short and long routes in the reduced-area design. We compare the interconnect complexity in the reduced-area design with that in the original design. Parameters we compare include: total measured netlength L_T, total Steiner length L_{TS}, total Manhattan length L_{TM}, excess Steiner length ΔL_{TS}, excess Manhattan length ΔL_{TM}, total number of vias v_T, total number of single stacked vias SSV, double stacked vias DSV, and triple stacked vias

TSV.

We compare the quality of the interconnections in the reduced-area design with the quality of interconnections in the original design. Measures of interconnect quality include: (1) Steiner quality Q_S, which is the ratio of the total Steiner length to *TESL*, as given by the expression,

$$Q_S = \frac{L_S}{\Delta L_{TS}}; \tag{59}$$

(2) Manhattan quality Q_M, which is the ratio of the total Manhattan length to *TEML*, as given by the expression,

$$Q_M = \frac{L_M}{\Delta L_{TM}}; \tag{60}$$

(3) number of vias per signal route.

A comparison of cumulative interconnect properties between the reduced-area design and the original design is then obtained. These properties include: (1) the total length L_T, (2) total route length (including power and ground), (3) needed route fraction L_T/L_{avail}, (4) area A_{int}, (5) total number of vias v_T, and (6) average number of vias per signal route v_T/N. The interconnect properties in both the reduced-area design and the original design are also compared on a layer-by-layer basis.

A.1 Application to the POWER4 IFU

In the POWER4 IFU study presented here, the IFU design area is reduced approximately 3% from the DD1 IFU area to the DD2 IFU area. The procedure to route the DD2 IFU is summarized in[21]. Table III lists signals routed with custom interconnections in the DD2 IFU. The total number of signals with custom interconnections N_c^i and the number of additional signals with custom interconnections ΔN_c^i are shown for each trial i, where $\Delta N_c^i = N_c^i - N_c^{(i-1)}$. A total of 136 buses, and a total of 3428 signals, are routed either with complete custom interconnections or partial custom interconnections in the DD2 IFU. Of these signals, 3415 are bus signals, and 13 are control signals. Figure 7 shows the number of route violations (shorts and design rule violations) in the DD2 IFU as a function of N_c (lower abscissa) and N_c/N (upper abscissa).

Figure 8 shows the CPU runtime as a function of N_c (lower abscissa) and N_c/N (upper abscissa). For each value of N_c, the DD2 IFU is routed with under the same conditions: (1)

the machine is an IBM RS/6000 Model397 with 1024M memory and AIX4.1.5 operating system; (2) the automated router is SiliconEnsemble version 5.2.109; (3) the automated route engine is WarpRoute version 2.1.23.1; (4) the route process incorporates the same set of three route configuration files, with one file per route stage. The configuration file for the first route stage sets parameters to route the design, the configuration file for the second stage sets parameters to repair routes with violations, and the configuration file for the third stage sets parameters to clean up remaining route violations, if possible. The CPU route runtime for each stage is denoted as CPU_1, CPU_2, and CPU_3, respectively; the total CPU runtime is CPU_{total}, and $CPU_{total} = CPU_1 + CPU_2 + CPU_3$. Figure 8 shows that CPU_{total} increases 4.4% when $N_c/N = 0.37$ compared with CPU_{total} when $N_c/N = 0$. The CPU runtime of each stage CPU_1, CPU_2, and CPU_3 remain nearly constant as N_c increases.

Figure 9 shows (a) the average fraction f_s of upper-level metal that routes short signals with $L \leq 0.7mm$ and (b) the average fraction of f_l of upper-level metal that routes long signals with $L \geq 0.7mm$, respectively, as a function of N_c. Figure 9(a) shows that f_s is reduced to approximately 92% when short targeted buses are completely routed and that f_s that routes remaining non-custom interconnections increases slightly as N_c increases. Figure 9(b) shows that f_l increases slightly with N_c for both long custom interconnections and long non-custom interconnections. These results are consistent with the results obtained for the DD1 IFU.

Table IV shows L_T, L_{TS}, L_{TM}, ΔL_{TS}, ΔL_{TM}, v_T, number of custom-routed signals N_c and the number of non-custom-routed signals N_r in both DD1 IFU and DD2 IFU designs. The table shows that ΔL_{TS}, ΔL_{TM}, and v_T are reduced for signals that are targeted to be custom-routed in DD2 compared with DD1. For custom interconnections, L_T increases slightly in DD2 because twenty-seven additional signals are custom-routed compared with DD1. For the rest of the routes, L_T and v_T are reduced. The total length L_T is reduced slightly because the macros are more tightly packed in the smaller DD2 IFU. The total number of vias v_T is reduced greatly because the via cost specified for the automatic router is increased in the DD2 IFU, as discussed later. ΔL_{TS} and ΔL_{TM} are greater in DD2 because the reduction in L_T is less than the reduction in available route length.

Table V shows *SSV*, *DSV*, and *TSV* for the DD2 IFU for each trial i as N_c is increased in the design. The table shows that custom interconnections reduce *SSV* by 31% from 5868 to 4034, *DSV* by 37% from 619 to 387, and *TSV* slightly from 6 to a single *TSV*.

Table IV compares the measures of quality discussed above in the DD1 IFU and DD2 IFU. The table shows that Q_S for custom interconnections increases more than 100% from 95.1 in DD1 to 211.8 in DD2, while Q_S for the rest of the routes decreases 25% from 98.1 in DD1 to 73.8 in DD2 because L_{TS} decreases and ΔL_{TS} increases. The table also shows that Q_M for custom interconnections increases 40% from 47.1 in DD1 to 65.5 in DD2, while Q_M for the rest of the routes decreases 13% from 50.9 in DD1 to 43.4 in DD2 because L_{TM} decreases and ΔL_{TM} increases. Table IV also shows that the number of vias per signal for signals targeted for custom interconnections (v_T/N_c, where in this case v_T represents the total number of vias in routes for signals targeted for custom interconnections) is reduced from 3.2 in DD1 to 3.1 in DD2. This table also shows that the number of vias per signal for the remaining signals that are routed with the automated router (v_T/N_r, where v_T represents in this case the total number of vias in the remaining routes) is reduced by nearly 1 via per signal (12%), from 7.3 in DD1 to 6.4 in DD2.

The cumulative interconnect properties are summarized in Table VII, which shows that the ratio of L_T to the minimum feature size ($0.18\mu m$) is 3.1×10^7. The total interconnect length (excluding power and ground) L_T and total number of vias v_T are reduced by 2% and 11%, respectively, from DD1 to DD2. The average number of vias per signal route v_T/N, another measure of interconnection quality[24], is reduced from 5.8 in DD1 to 5.2 in DD2. The needed route fraction is obtained from Table VI and Table VII as the ratio of the total route length L_T to L_{avail}. Table VII shows that the needed route fraction increases slightly from 18% in DD1 to 19% in DD2. For both versions of the IFU in DD1 and DD2, the values of the needed route fraction are well below the suggested 40% limit[8] for the wirability of high-performance CMOS microprocessors. However, despite the fact that these average values of the needed route fraction indicate that the IFU is easily wirable, there do exist three localized regions of the IFU that are wirable only after instantiation of custom interconnections, as discussed previously.

For a layer-by-layer comparison of the DD1 IFU and DD2 IFU, Table VIII shows the to-

tal available interconnect length L_{avail}, total interconnect length L_T, and fraction L_T/L_{avail} of available interconnect needed to route unit-level IFU signals on each metal layer. The table shows that metal layers *m3* and *m4* have the longest length available to route minimum-width wires. Approximately $20\% - 25\%$ of the available interconnect length on each upper-level metal layer routes interconnections. Table IX shows the total number of vias v_T that routes unit-level interconnections. The table shows that more than 50% of the vias connect *m3* and *m4* on layer *v3* in the DD1 and DD2, and that the total number of vias v_T required to route the design decreases 11% to 48197 in DD2 from 53562 in DD1, which results from specifying higher via cost for the automated router WarpRoute. WarpRoute completes routes of the remaining signals with specified cost factors for each via layer and metal layer for both straight routes and wrong-way routes (e.g., horizontal *m4*).

B. Impact of via and metal cost choices for the automated router

Another technique to optimize physical properties of design interconnections is to optimize results generated by the automated router. In one possible scenario, the first step is to obtain a design that contains all desired custom interconnections, if applicable, and is routed with zero violations. The next step is to increase the route costs of the lower-level metal layers (namely, c_{m1} and c_{m2}) relative to the costs of the upper-level metal layers (c_{m3}, c_{m4}, c_{m5}) in the appropriate route configuration file. With this choice of costs, the automated router is instructed to route preferentially unit-level signals on upper-level metal. Next, the design is routed, and the total number of vias and total interconnect length are measured. The metal costs are increased and the design is routed until either route violations are observed or until the total interconnect length is no longer reduced. At this point, the metal costs of the last trial with zero route violations and smallest value of total netlength are chosen as metal costs to optimize route results. Next, the via costs for each via layer, c_{v1} through c_{v4}, are increased. The design is routed and the total number of vias is obtained. Via costs are increased, and the design is rerouted, until route violations occur or until the total number of vias in unit-level signals is no longer reduced. At this point, the via costs of the last trial with zero route violations and smallest via number are chosen as via costs to optimize the design results.

B.1 Application to the POWER4 IFU

Table X presents an overview of the total number of vias v_T in unit-level interconnections in the DD1 IFU ($N_c = 3401$) and DD2 IFU ($N_c = 3428$). The numbers shown in boldface are the numbers of vias in the DD1 IFU (for which $v_T = 53562$) and DD2 IFU (for which $v_T = 48194$), respectively. To generate the values shown in this table, the cost parameters of each via layer (c_{v1} through c_{v4}) and each metal layer (c_{m1} through c_{m5}) for regular routes and wrong-way routes are set to the series of values shown. Table X shows that the number of vias in unit-level signals decreases as the via cost increases, as shown for trials a through e, and decreases as the metal cost decreases with constant via cost (trials c through h). When the via costs are too high, the number of electrical shorts s and number of unrouted signals $N_{unroutes}$ become large. For the DD2 IFU, the automated router routes a design with zero shorts $s = 0$ with $\{c_{v1}, c_{v2}, c_{v3}, c_{v4}\} = 8$. Since this value exceeds $\{c_{v1}, c_{v2}, c_{v3}, c_{v4}\} = 4$ in the DD2 IFU, we conclude that v_T could have been reduced an additional 6.4% compared with that in the DD2 IFU (equivalently, 15.8% compared with that in the DD1 IFU).

Table XI shows an overview of the ratios r_a and r_c of length to vias instantiated by the automated router and by custom interconnections, respectively, as well as the fraction f_{12} of lower-level metal and the fraction f_{345} of upper-level metal in the DD1 IFU and DD2 IFU obtained with different values of the cost parameters $\{c_{v_j}\}$ ($j = 1$ through 4) for the via layers *v1,v2,v3,v4* and cost parameters $\{c_{v_k}\}$ ($k = 1$ through 5) for the metal layers *m1,m2,m3,m4,m5*. The fractions f_{12} and f_{345} are given by the expressions $f_{12} = (L_{m1} + L_{m2})/(L_{m1} + L_{m2} + L_{m3} + L_{m4} + L_{m5})$ and $f_{345} = (L_{m3} + L_{m4} + L_{m5})/(L_{m1} + L_{m2} + L_{m3} + L_{m4} + L_{m5})$, respectively, where the terms L_{m1} through L_{m5} represent the route length per metal layer. The table shows that as the via costs are increased, r_a increases from approximately $75\mu m$ per via to approximately $120\mu m$ per via for the DD1 and DD2 designs; and that f_{12} increases from 0.010 to 0.014 while f_{345} decreases from 0.99 to 0.986. The ratio r_a is as high as $133\mu m$ per via when the metal costs are smallest (trial h), which also produces the largest $f_{12} = 0.13$ and smallest $f_{345} = 0.87$. The ratio r_c for the instantiated custom interconnections remains constant with changing cost values at 255 μm per via (DD1 IFU) and 219 μm per via (DD2 IFU) since the same set of custom

interconnections is in each trial. As in Table X, the numbers shown in boldface indicate the values obtained in the DD1 IFU and DD2 IFU, respectively.

Table XII shows an overview of the number of stacked vias in DD1 IFU and DD2 IFU signal routes. The stacked vias include single stacked vias *SSV*, double stacked vias *DSV*, and triple stacked vias *TSV* as a function of different values of the cost parameters $\{c_{v_j}\}$ ($j = 1$ through 4) for the via layers *v1,v2,v3,v4* and cost parameters $\{c_{v_k}\}$ ($k = 1$ through 5) for the metal layers *m1,m2,m3,m4,m5*. The table shows the values of the cost parameters c_{m1} and c_{m2} for routes on lower-level metal and the cost parameters c_{m3}, c_{m4}, c_{m5} for regular (*reg*) and wrong-way (*perp*) routes on upper-level metal. The numbers shown in boldface indicate the values obtained in the DD1 IFU and DD2 IFU, respectively. The table shows that the values for *SSV*, *DSV*, *TSV* are significantly reduced as the via costs are increased from 1 in trial *a* to 32 in trial *e*. The values for *SSV*, *DSV*, and *TSV* are reduced 64% in DD1 and 54% in DD2 for trial *h*, in which the via costs are 8 and the metal route costs are set to their minimum value (i.e., 1).

IV. Conclusions

Analytical techniques to quantify the quality of custom interconnections and to optimize interconnections in a ULSI design are presented. These techniques provide designers with useful tools to help decide whether a proposed pre-route algorithm has a positive impact on the overall design process.

Acknowledgments

We thank Pong-Fei Lu, Robert Wisniewski, and Mike Rosenfield of the IBM T. J. Watson Research Center, Yorktown Heights, NY, and Brian Konigsburg at IBM Server Division in Austin, TX, for their comments on the text.

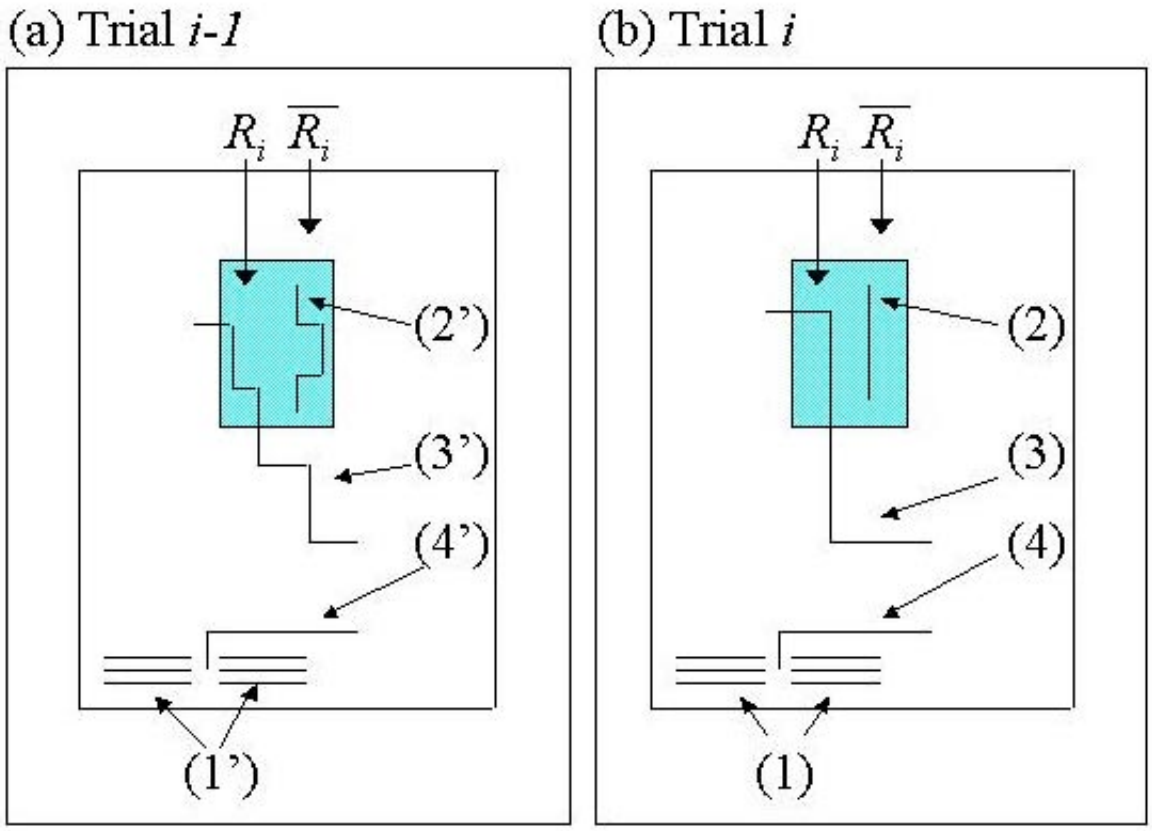

Fig. 1. Comparison of design routes in trial i (b) with routes in trial $i-1$ (a). R_i is shaded blue, and $\overline{R}_i$ is unshaded. (1') and (1) show the custom interconnections inserted in trial *i-1* and trial i with total length $L_c^{(i-1)}$; (2') shows targeted routes in R_i with length $\Delta L_t^{(i-1)}$; (2) shows custom interconnections in R_i with length $\Delta L_c^{(i-1)}$; (3') shows routes that partially pass through R_i in trial $i-1$ with length $L_o^{(i-1)}$; (3) shows routes that partially pass through R_i in trial i with total length $L_o^{(i)}$; (4') and (4) show remaining routes that do not pass through R_i with total length $L_r^{(i-1)}(\overline{R_i})$ and $L_r^{(i)}(\overline{R_i})$, respectively, in trials $i-1$ and i.

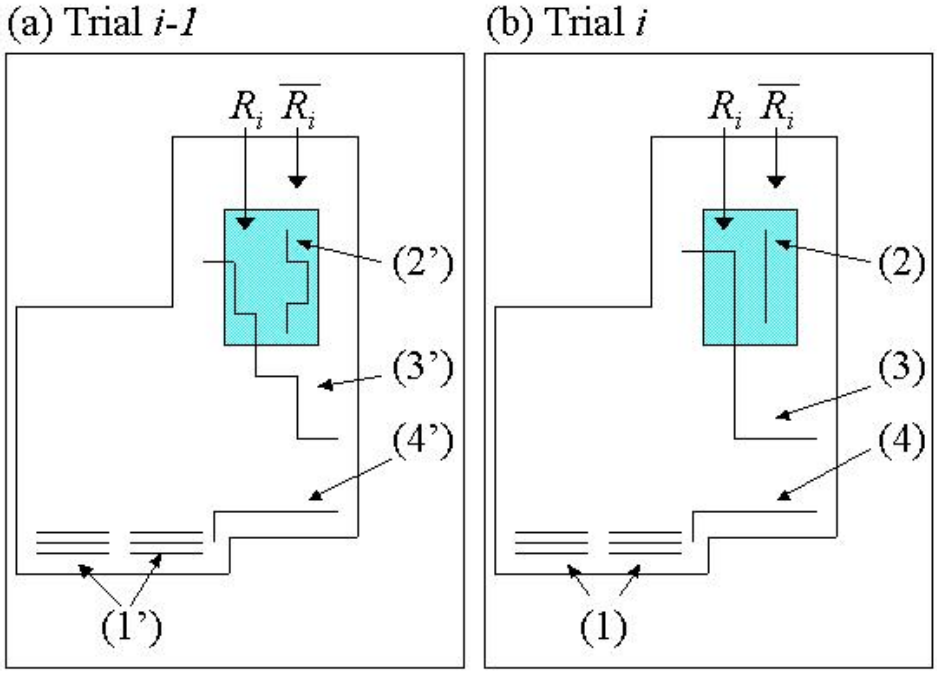

Fig. 2. Schematic of Fig. 1 applied to the case of the IFU floorplan. In this case, R_i is shaded blue, and $\overline{R}_i$ is unshaded. As in Fig. 1, (1') and (1) show custom interconnections inserted in both trials $i-1$ and i with total length $L_c^{(i-1)}$; (2') shows targeted routes in R_i with length $\Delta L_t^{(i-1)}$; (2) shows custom routes in R_i with length $\Delta L_c^{(i-1)}$; (3') shows routes that partially pass through R_i in trial $i-1$ with length $L_o^{(i-1)}$; (3) shows routes that partially pass through R_i in trial i with total length $L_o^{(i)}$; (4') and (4) show remaining routes that do not pass through R_i with total length $L_r^{(i-1)}(\overline{R_i})$ and $L_r^{(i)}(\overline{R_i})$, respectively, in trials $i-1$ and i.

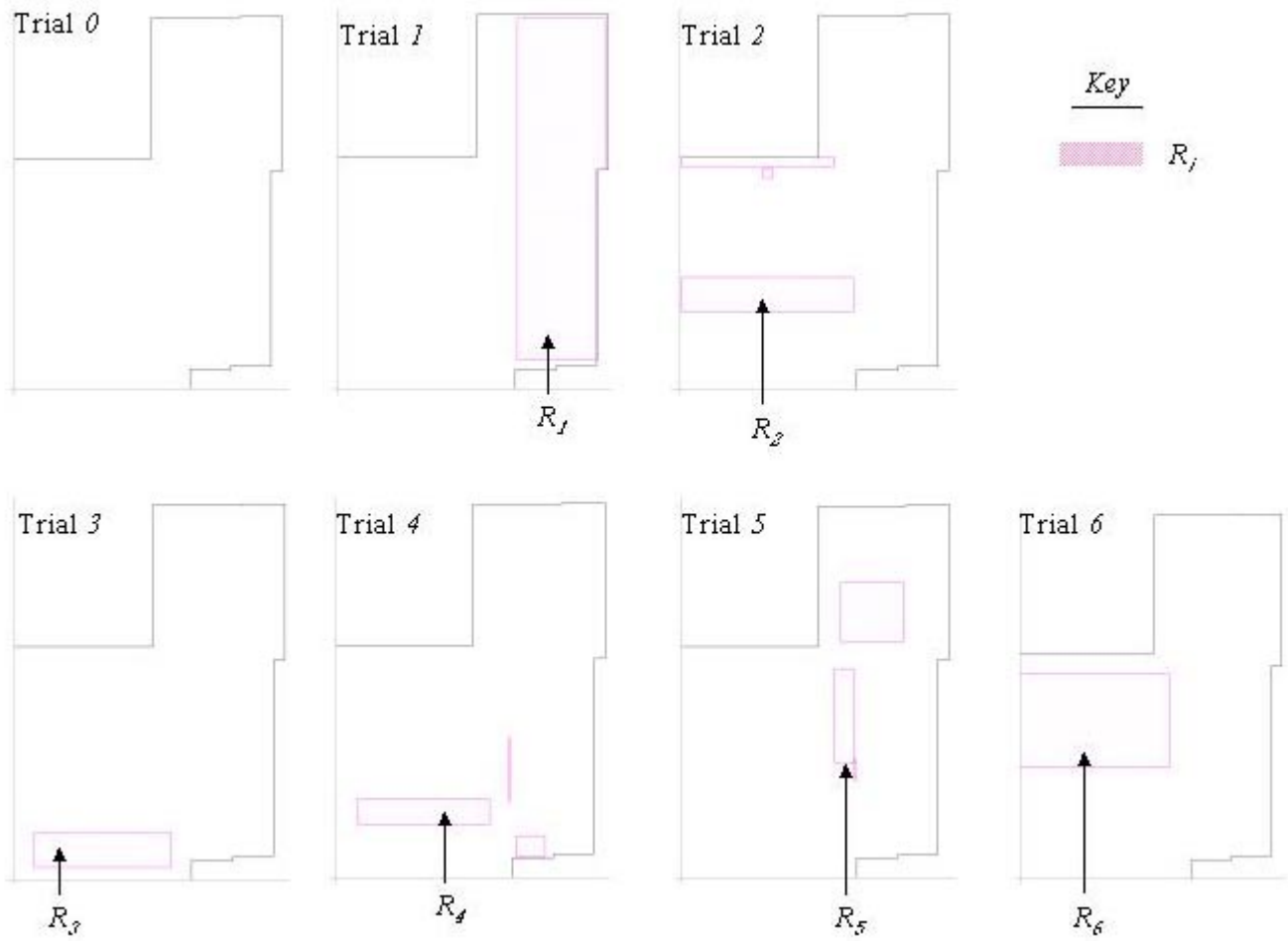

Fig. 3. R_i in each of the six routing trials in the DD1 IFU. R_i is shown as the shaded region in each trial.

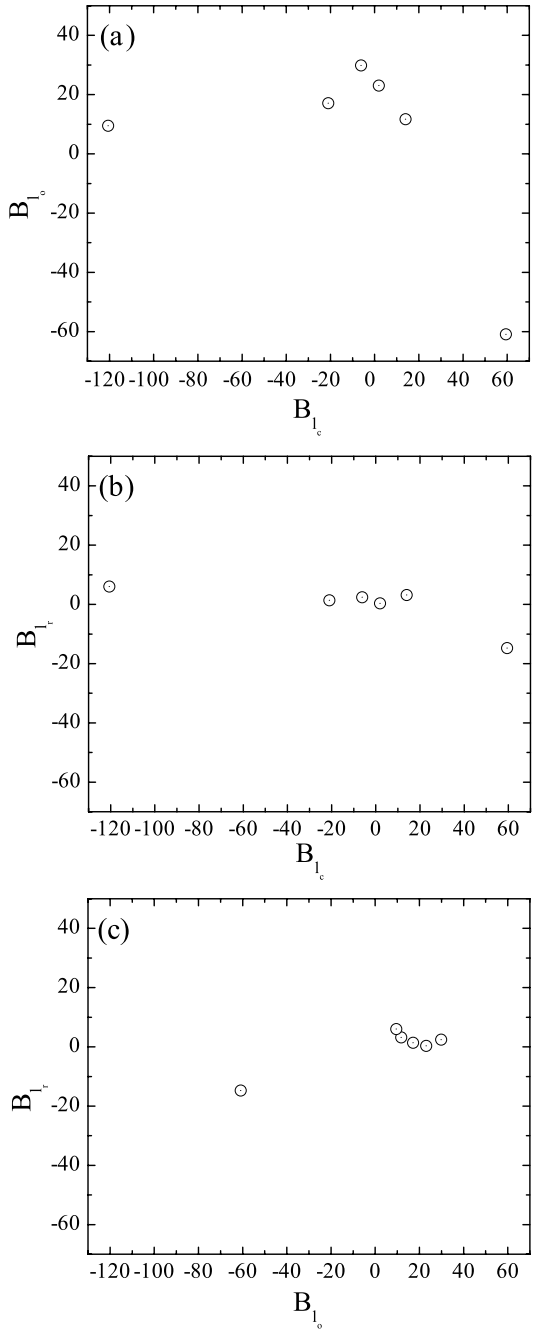

Fig. 4. Scatterplots of *B-values* for netlengths in the DD1 IFU: (a) $\{B^{(i)}_{L_o}\}$ versus $\{B^{(i)}_{L_c}\}$, (b) $\{B^{(i)}_{L_r}\}$ versus $\{B^{(i)}_{L_c}\}$, and (c) $\{B^{(i)}_{L_r}\}$ versus $\{B^{(i)}_{L_o}\}$ for lengths of custom routes (L_c), lengths of other routes (L_o) that pass through R_i, and lengths of the rest of routes (L_r) that do not pass through R_i.

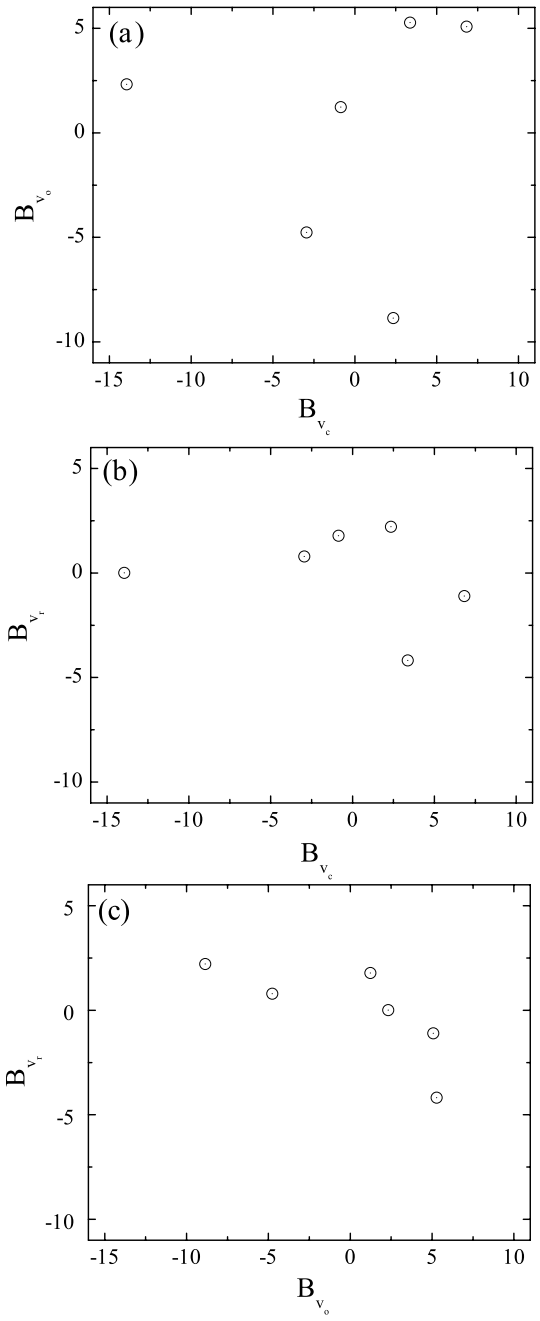

Fig. 5. Scatterplots of *B-values* for vias in the DD1 IFU: (a) $\{B_{v_o}^{(i)}\}$ versus $\{B_{v_c}^{(i)}\}$, (b) $\{B_{v_r}^{(i)}\}$ versus $\{B_{v_c}^{(i)}\}$, and (c) $\{B_{v_r}^{(i)}\}$ versus $\{B_{v_o}^{(i)}\}$ for vias in custom routes (v_c), other routes (v_o) that pass through R_i, and the rest of routes (v_r) that do not pass through R_i.

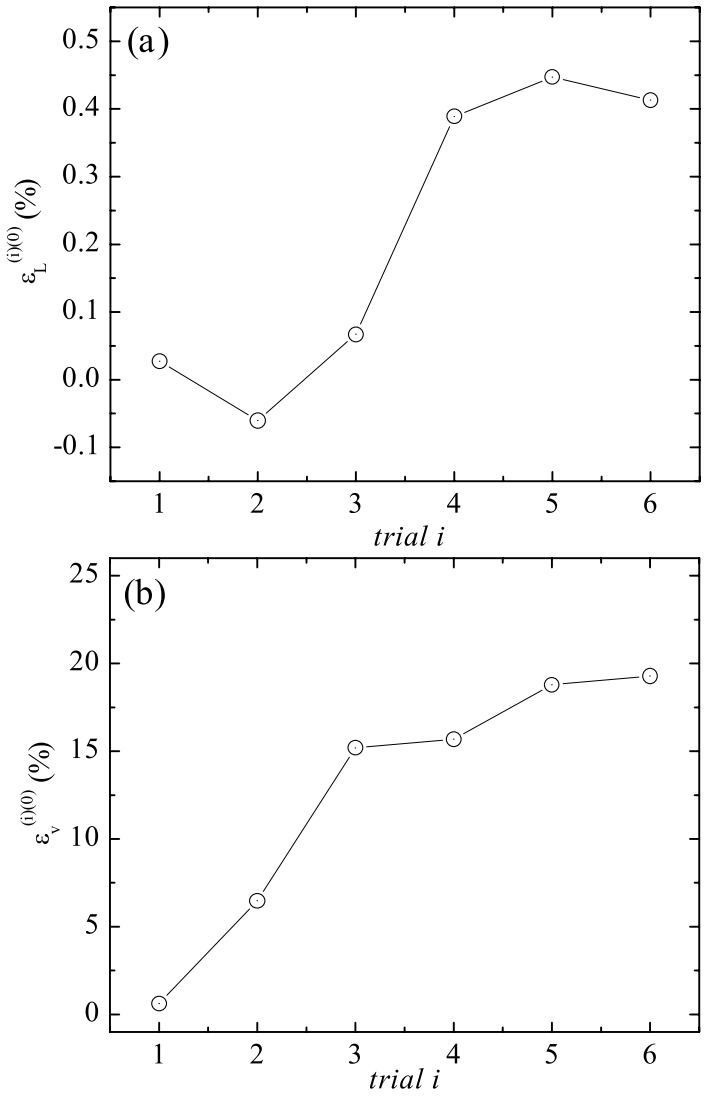

Fig. 6. Measured cumulative effectiveness for (a) netlengths $\epsilon_L^{(i)(0)}$ and (b) vias $\epsilon_v^{(i)(0)}$ in the DD1 IFU for each trial i.

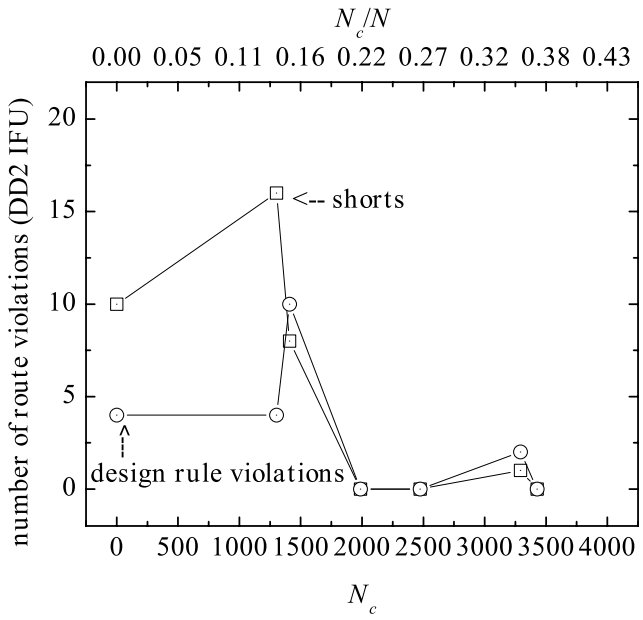

Fig. 7. Route violations in the DD2 IFU. Design rule violations (circles) and electrical shorts (squares) are shown.

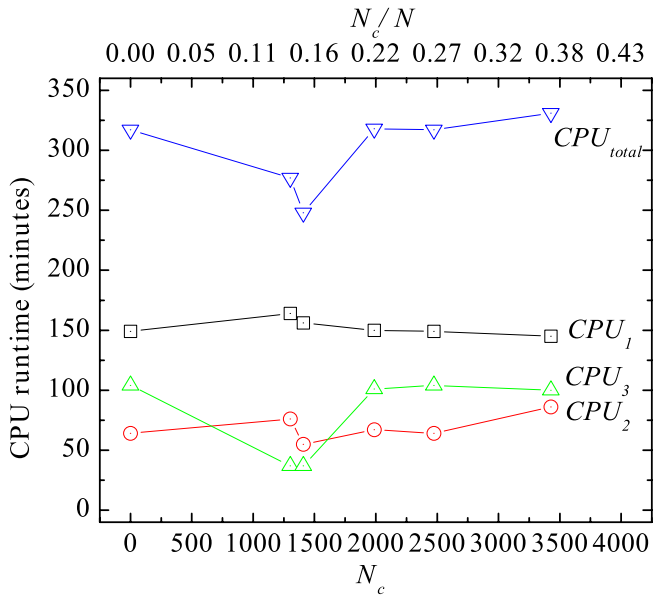

Fig. 8. CPU runtime in DD2 IFU as a function of N_c (lower abscissa) and N_c/N (upper abscissa). The total CPU runtime CPU_{total} (blue triangles) is the sum of each runtime required for each of the three route phases, namely $CPU_{total} = CPU_1 + CPU_2 + CPU_3$. Also shown are the CPU runtimes for the first route stage CPU_1 (black squares), second stage CPU_2 (red circles), and third stage CPU_3 (green triangles).

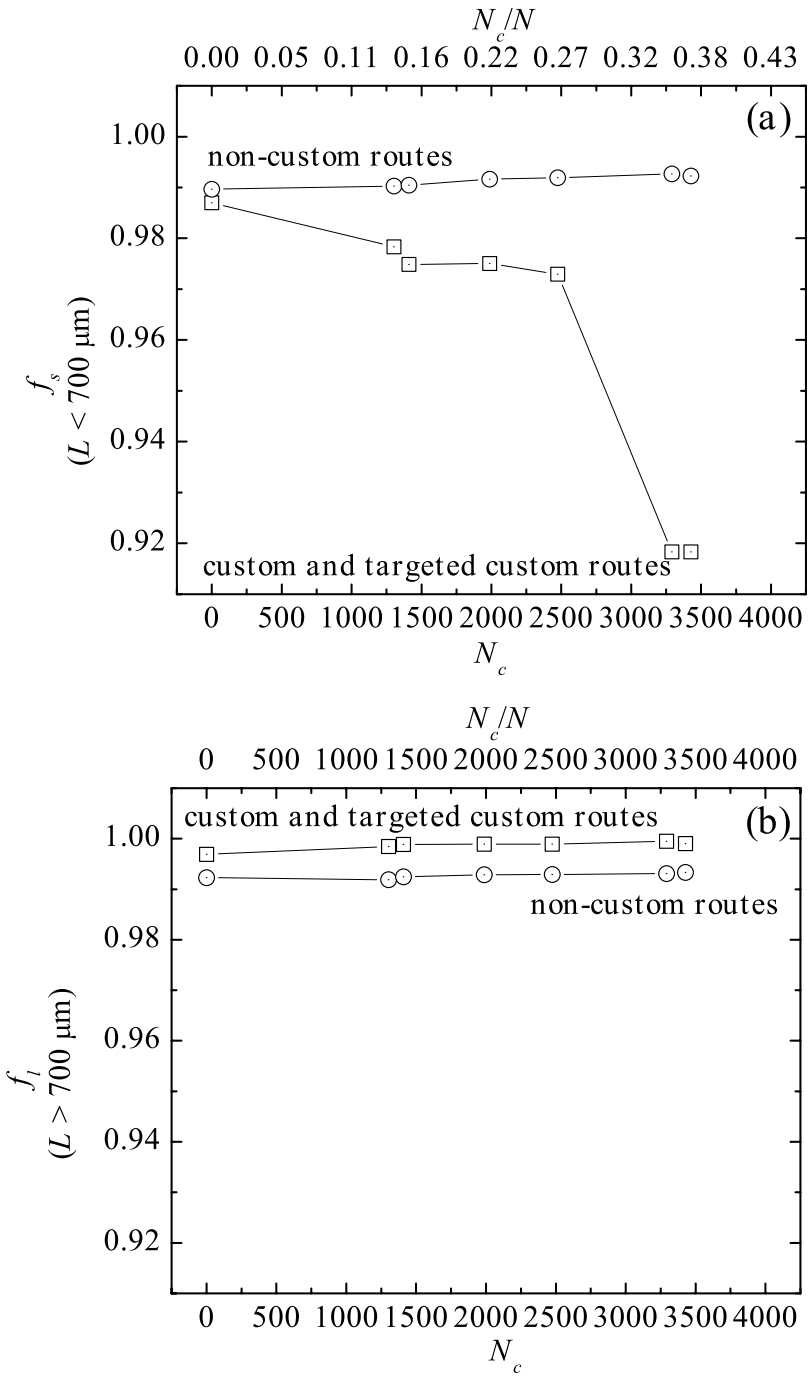

Fig. 9. Fraction of upper-level metal in DD2 IFU (a) short and (b) long routes as a function of the number (fraction) of custom interconnections N_c (lower abscissa) and N_c/N (upper abscissa).

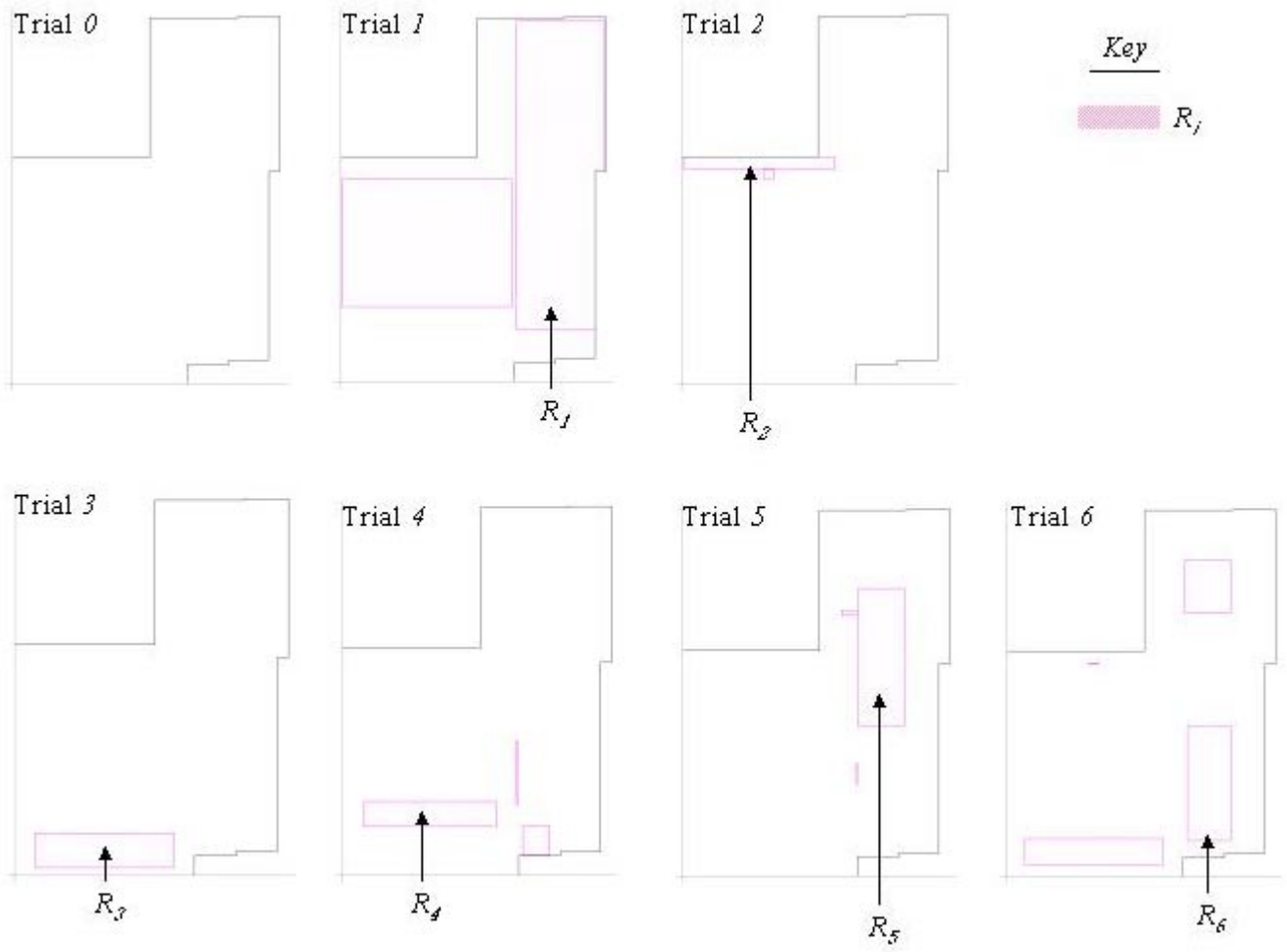

Fig. 10. R_i in each of the six routing trials in the DD2 IFU. R_i is shaded in each trial.

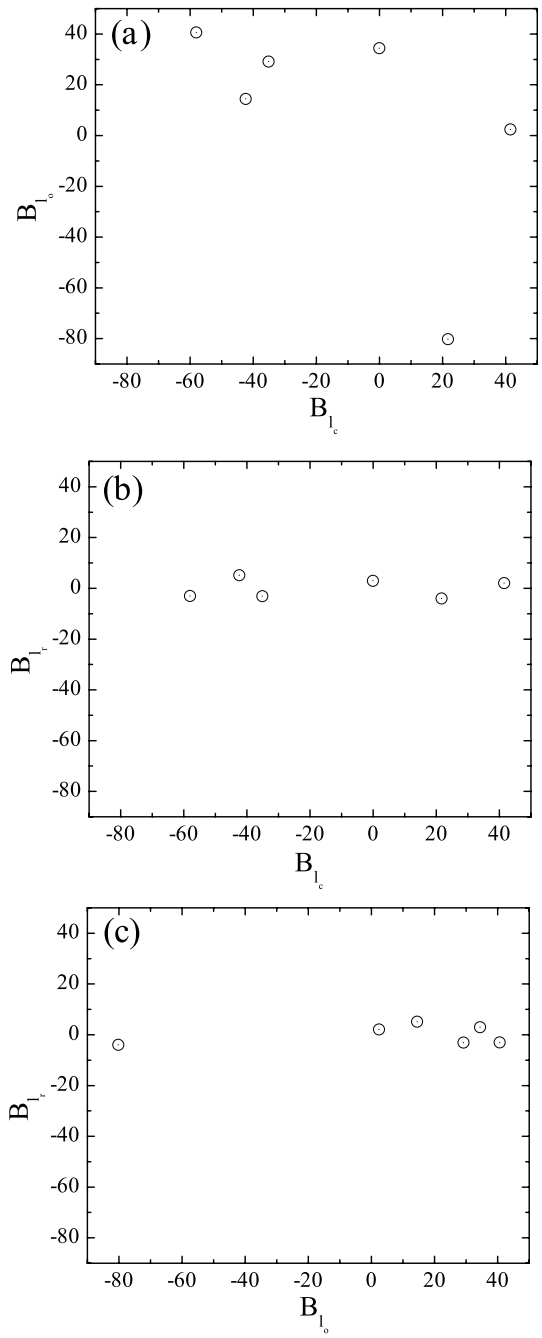

Fig. 11. Scatterplots of *B-values* in DD2 design for netlengths (a) $\{B^{(i)}_{L_o}\}$ versus $\{B^{(i)}_{L_c}\}$, (b) $\{B^{(i)}_{L_r}\}$ versus $\{B^{(i)}_{L_c}\}$, and (c) $\{B^{(i)}_{L_r}\}$ versus $\{B^{(i)}_{L_o}\}$ (c) for lengths of custom interconnections (L_c), lengths of other routes (L_o) that pass through R_i, and lengths of the rest of routes (L_r) that do not pass through R_i.

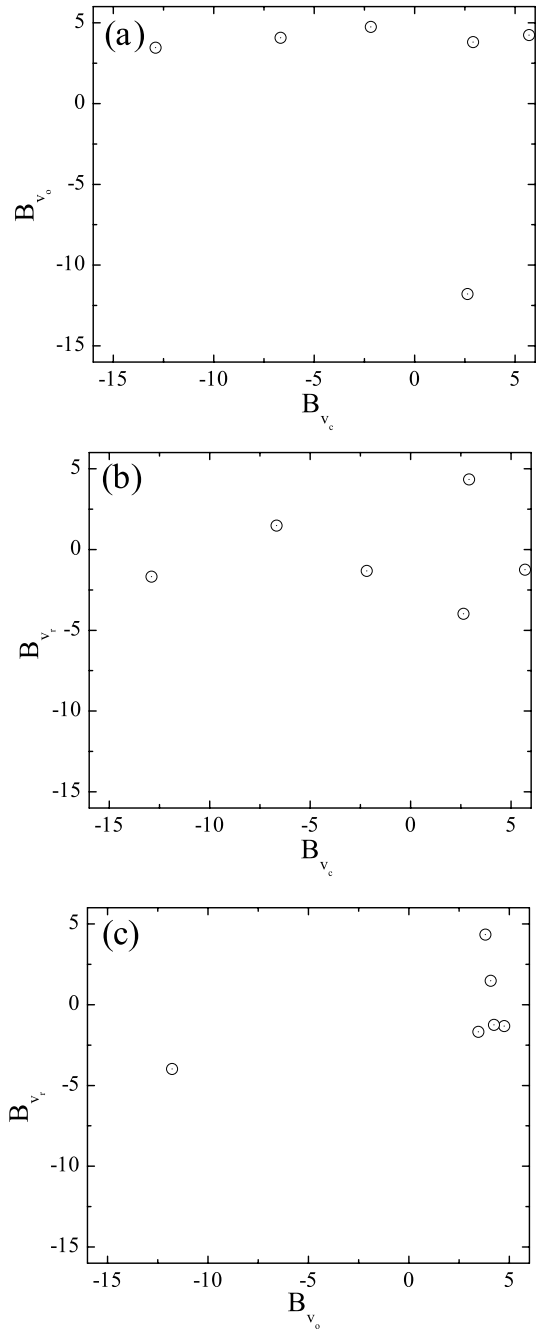

Fig. 12. Scatterplots of *B-values* in DD2 design for vias (a) $\{B_{v_o}^{(i)}\}$ versus $\{B_{v_c}^{(i)}\}$, (b) $\{B_{v_r}^{(i)}\}$ versus $\{B_{v_c}^{(i)}\}$, and (c) $\{B_{v_r}^{(i)}\}$ versus $\{B_{v_o}^{(i)}\}$ for vias in custom routes (v_c), other routes (v_o) that pass through R_i, and the rest of routes (v_r) that do not pass through R_i.

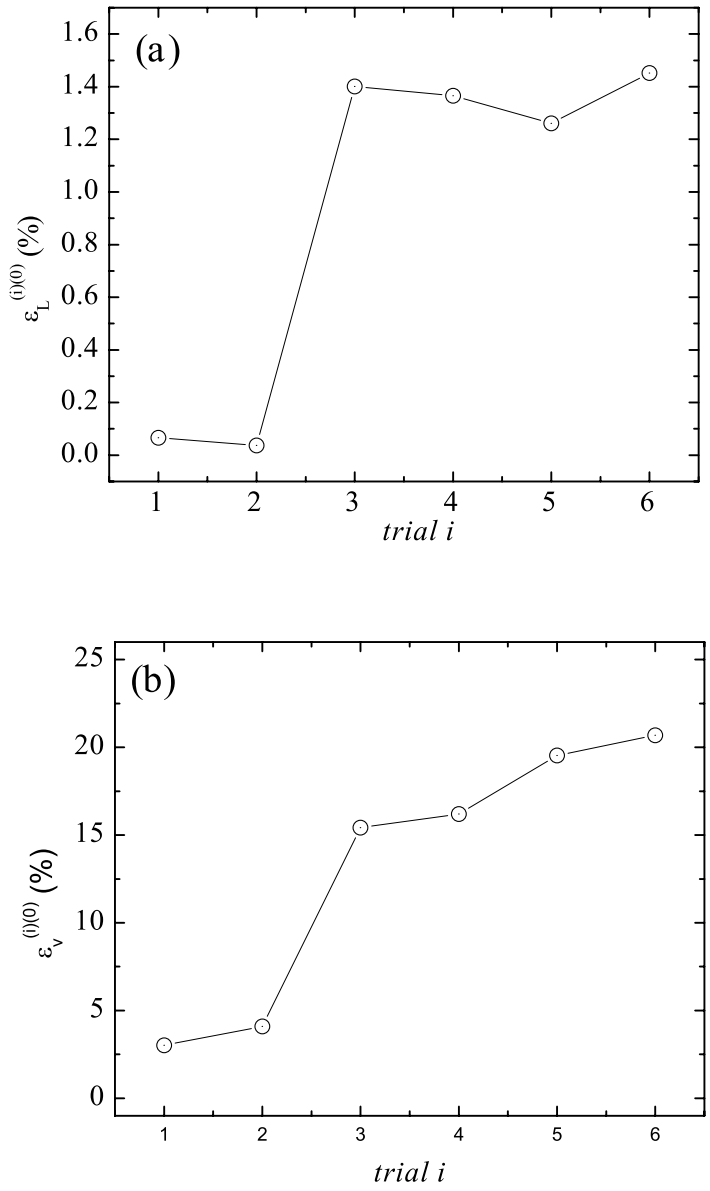

Fig. 13. Measured cumulative effectiveness (a) for netlengths $\epsilon_L^{(i)(0)}$ and (b) vias $\epsilon_v^{(i)(0)}$ in the DD2 IFU for each trial i.

TABLE I

INTERCONNECT EFFECTIVENESS IN THE DD1 IFU. FOR NETLENGTHS L: $\epsilon_{L_c}^{(i)}$, $\epsilon_{L_o}^{(i)}$, $\epsilon_{L_r}^{(i)}$, $\epsilon_{L}^{(i)}$, WITH THE CORRESPONDING VALUES FOR $p_{L_t}^{(i-1)}$, $p_{L_o}^{(i-1)}$, $p_{L_r}^{(i-1)}$ AND $\Delta L_t^{(i-1)}$, $L_o^{(i-1)}$, AND $L_r^{(i-1)}$. $\Delta L_t^{(i-1)}$, $L_o^{(i-1)}$, AND $L_r^{(i-1)}$ ARE EXPRESSED IN UNITS OF *meters*. THE VALUES FOR $\epsilon_{L_c}^{(i)}$, $\epsilon_{L_o}^{(i)}$, $\epsilon_{L_r}^{(i)}$ AND $\epsilon_{L}^{(i)}$ ARE GIVEN IN %. FOR VIAS V: $\epsilon_{v_c}^{(i)}$, $\epsilon_{v_o}^{(i)}$, $\epsilon_{v_r}^{(i)}$, AND $\epsilon_{v}^{(i)}$ WITH THE CORRESPONDING VALUES FOR $p_{v_t}^{(i-1)}$, $p_{v_o}^{(i-1)}$, $p_{v_r}^{(i-1)}$, AND $\Delta v_t^{(i-1)}$, $v_o^{(i-1)}$, AND $v_r^{(i-1)}$. THE VALUES FOR $\epsilon_{v_c}^{(i)}$, $\epsilon_{v_o}^{(i)}$, $\epsilon_{v_r}^{(i)}$, AND $\epsilon_{v}^{(i)}$ ARE GIVEN IN %.

L	*custom interconnections in* R_i			*other routes in* R_i			*rest of routes in* $\overline{R}_i$			*all routes*	
i	$\epsilon_{L_c}^{(i)}(\%)$	$p_{L_t}^{(i-1)}$	$\Delta L_t^{(i-1)}$	$\epsilon_{L_o}^{(i)}(\%)$	$p_{L_o}^{(i-1)}$	$L_o^{(i-1)}$	$\epsilon_{L_r}^{(i)}(\%)$	$p_{L_r}^{(i-1)}$	$L_r^{(i-1)}$	$\epsilon_{L}^{(i)}(\%)$	$L^{(i-1}$
1	9.2	0.19	1.05	−4.5	0.32	1.78	−0.57	0.49	2.68	0.027	5.51
2	7.0	0.036	0.163	−1.3	0.25	1.14	−0.064	0.71	4.20	−0.11	5.51
3	7.7	0.12	0.52	−0.19	0.023	0.100	0.013	0.86	3.78	0.92	5.51
4	−13.0	0.033	0.13	−1.2	0.061	0.24	0.099	0.91	3.53	−0.40	5.47
5	5.3	0.016	0.061	0.0043	0.13	0.50	−0.0012	0.85	3.20	0.086	5.49
6	−4.3	0.063	0.23	−1.4	0.23	0.83	−0.026	0.71	2.64	0.051	5.48

V	*custom interconnections in* R_i			*other routes in* R_i			*rest of routes in* $\overline{R}_i$			*all routes*	
i	$\epsilon_{v_c}^{(i)}(\%)$	$p_{v_t}^{(i-1)}$	$\Delta v_t^{(i-1)}$	$\epsilon_{v_o}^{(i)}(\%)$	$p_{v_o}^{(i-1)}$	$v_o^{(i-1)}$	$\epsilon_{v_r}^{(i)}(\%)$	$p_{v_r}^{(i-1)}$	$v_r^{(i-1)}$	$\epsilon_{v}^{(i)}(\%)$	$v^{(i-1}$
1	69	0.12	7630	−1.7	0.40	26210	−2.1	0.49	32515	6.2	6635
2	59	0.034	2016	−7.3	0.27	16109	0.44	0.70	41730	0.34	6225
3	65	0.14	8327	−0.52	0.020	1162	0.80	0.84	49339	9.8	6205
4	25	0.022	1119	0.66	0.046	2290	0.088	0.93	46702	0.67	5627
5	78	0.055	2682	2.7	0.10	5048	−0.41	0.84	41206	4.2	5594
6	73	0.021	976	−16	0.11	5181	1.1	0.87	40129	0.71	5389

TABLE II

INTERCONNECT EFFECTIVENESS IN THE IFU DD1. THE *mean effectiveness*, *standard error*, *p-value*, *lower confidence bound LCB*, AND *upper confidence bound UCB* ARE SHOWN FOR CUSTOM INTERCONNECTIONS, THE OTHER ROUTES, AND THE REST OF THE ROUTES. THE CONFIDENCE INTERVALS HAVE 95% COVERAGE; FOR μ_{L_c} AND μ_{v_c}, ONLY THE LOWER 95% BOUND IS GIVEN.

Netlengths	*mean(%)*	*std. error(%)*	*p-value*	$LCB(\%)$	UC
custom interconnections	$\tilde{\mu}_{L_c} = 6.7$	$\hat{\sigma}(\hat{\mu}_{L_c}) = 2.3$	$p\text{-}value(\mu_{L_c}) = 0.015$	2.2	
other routes	$\tilde{\mu}_{L_o} = -2.4$	$\hat{\sigma}(\hat{\mu}_{L_o}) = 0.85$	$p\text{-}value(\mu_{L_o}) = 0.039$	-4.5	-0
rest of routes	$\tilde{\mu}_{L_r} = -0.074$	$\hat{\sigma}(\hat{\mu}_{L_r}) = 0.091$	$p\text{-}value(\mu_{L_r}) = 0.46$	-0.31	0.
Vias	*mean(%)*	*std. error(%)*	*p-value*	$LCB(\%)$	UC
custom interconnections	$\tilde{\mu}_{v_c} = 65.4$	$\hat{\sigma}(\hat{\mu}_{v_c}) = 4.4$	$p\text{-}value(\mu_{v_c}) = 0.000013$	56.5	
other routes	$\tilde{\mu}_{v_o} = -4.1$	$\hat{\sigma}(\hat{\mu}_{v_o}) = 2.2$	$p\text{-}value(\mu_{v_o}) = 0.12$	-9.7	1
rest of routes	$\tilde{\mu}_{v_r} = 0.085$	$\hat{\sigma}(\hat{\mu}_{v_r}) = 0.43$	$p\text{-}value(\mu_{L_r}) = 0.85$	-1.0	1

TABLE III

OVERVIEW OF CUSTOM INTERCONNECTIONS IN THE DD2 IFU. THE NUMBER OF CUSTOM INTERCONNECTIONS N_c^i, NUMBER OF ADDITIONAL CUSTOM INTERCONNECTIONS ΔN_c^i, NUMBER OF BUS SIGNALS N_{bus}, AND NUMBER OF CONTROL SIGNALS $N_{control}$ ROUTED WITH CUSTOM INTERCONNECTIONS ARE SHOWN. ALSO SHOWN ARE THE NUMBER OF BUSES ROUTED IN EACH REGION N_{reg1} THROUGH N_{reg7}. THE TOTAL NUMBER OF BUSES IN ALL REGIONS N_{regtot} ARE ALSO SHOWN, WHERE $N_{regtot} = \sum_1^7 N_{reg_i}$.

.

i	N_c^i	ΔN_c^i	N_{bus}	N_{cntl}	N_{r1}	N_{r2}	N_{r3}	N_{r4}	N_{r5}	N_{r6}	N_{r7}	N_{rtot}
0	0	0	0	0	0	0	0	0	0	0	0	0
1	1303	1303	1303	0	0	17	0	0	16	0	0	33
2	1410	107	96	11	3	0	0	0	0	0	0	3
3	1988	578	578	0	0	0	42	0	0	0	0	42
4	2474	486	486	0	0	0	0	4	0	2	24	30
5	3291	817	817	0	0	23	0	1	0	0	0	24
6	3428	137	135	2	0	2	2	0	0	0	0	4
6	3428	3428	3415	13	3	42	44	5	16	2	24	136

TABLE IV

COMPARISON OF INTERCONNECT COMPLEXITY IN THE DD1 IFU AND DD2 IFU. THE TOTAL LENGTH L_T, TOTAL STEINER LENGTH L_{TS}, TOTAL MANHATTAN LENGTH L_{MT}, *TESL*, *TEML*, AND TOTAL NUMBER OF VIAS v_T ARE SHOWN FOR CUSTOM-ROUTED SIGNALS N_c AND NON-CUSTOM-ROUTED SIGNALS N_r. THE STEINER QUALITY Q_S, MANHATTAN QUALITY Q_M, AND AVERAGE NUMBER OF VIAS PER SIGNAL ARE ALSO SHOWN.

custom interconnections	*DD1*	*DD2*
L_T (m)	2.12	2.13
L_{TS} (m)	2.09	2.12
L_{TM} (m)	2.07	2.10
TESL (m)	0.02	0.01
TEML (m)	0.04	0.03
v_T	11007	10760
N_c	3401	3428
Q_S	95.1	211.8
Q_M	47.1	65.5
v_T/N_c	3.2	3.1
non-custom interconnections	*DD1*	*DD2*
L_T (m)	3.37	3.29
L_{TS} (m)	3.34	3.25
L_{TM} (m)	3.31	3.22
TESL (m)	0.03	0.04
TEML (m)	0.07	0.07
v_T	42555	37434
N_r	5852	5855
Q_S	98.1	73.8
Q_M	50.9	43.4
v_T/N_r	7.3	6.4

TABLE V

SINGLE STACKED VIAS *SSV*, DOUBLE STACKED VIAS *DSV*, TRIPLE STACKED VIAS *TSV* IN THE DD2 IFU FOR EACH TRIAL i, WHERE N_c IS SHOWN FOR EACH TRIAL. EACH *SSV* IS COMPOSED OF TWO STACKED VIAS; EACH *DSV* IS COMPOSED OF THREE STACKED VIAS; EACH *TSV* IS COMPOSED OF FOUR STACKED VIAS.

.

i	N_c	*SSV*	*DSV*	*TSV*
0	0	5868	619	6
1	1016	5445	555	9
2	1275	5315	559	9
3	1853	4456	517	6
4	2339	4459	392	3
5	3135	4024	418	4
6	3101	4034	387	1

TABLE VI

IFU PHYSICAL DESIGN CONSTRAINTS. THE UNIT AREA A, NUMBER N OF UNIT-LEVEL SIGNALS, OCCUPANCY O, AND TOTAL AVAILABLE LENGTH L_{avail} OF MINIMUM-WIDTH WIRE FOR UNIT-LEVEL SIGNALS ARE SHOWN.

.

Physical Design Constraints	*DD1*	*DD2*
unit width (μm)	3643.61	3643.61
unit height(μm)	5080.64	5010.08
A (mm^2)	14.1	13.8
number of IO pins	1723	1722
N	9253	9283
average signal fan-out	2.3	2.3
macros (including buffers and inverters)	999	1039
macros (not including buffers and inverters)	95	95
transistors ($\times 10^6$)	5.9	5.9
array transistors ($\times 10^6$)	4	4
buffers and inverters	904	944
O	0.81	0.85
L_{avail} *(meters)*	31.3	28.9
available route fraction	34%	31%

TABLE VII

OVERVIEW OF UNIT-LEVEL INTERCONNECTIONS IN DD1 IFU AND DD2 IFU. THE TOTAL LENGTH L_T OF WIRE, TOTAL AREA A_{int} OCCUPIED BY INTERCONNECT, TOTAL VIA NUMBER v_T, AND AVERAGE NUMBER OF VIAS PER SIGNAL v_T/N IN THE UNIT-LEVEL SIGNALS ARE SHOWN.

IFU Interconnect Results	*DD1*	*DD2*
L_T (m)	5.5	5.4
L_T *(incl. pwr, gnd)* (m)	17.0	16.5
needed route fraction L_T/L_{avail}	18%	19%
A_{int} *(incl. pwr, gnd)* (mm^2)	12.6	12.2
v_T	53562	48194
v_T/N	5.8	5.2

TABLE VIII

DETAILED INTERCONNECT CHARACTERISTICS FOR ALL N SIGNALS IN THE DD1 IFU AND DD2 IFU (EXCLUDING POWER AND GROUND). FOR OF THE FIVE AVAILABLE METAL LAYERS, THE AVAILABLE LENGTH L_{avail} OF MINIMUM-WIDTH WIRE, TOTAL WIRE LENGTH L_T, AND FRACTION OF AVAILABLE ROUTE RESOURCES FOR UNIT-LEVEL SIGNALS ARE SHOWN.

.

DD1 interconnections	*m1*	*m2*	*m3*	*m4*	*m5*	$m1-m5$
L_{avail} (m)	4.53	3.41	7.39	13.2	2.75	31.3
L_T (m)	0.020	0.037	1.46	3.35	0.621	5.5
needed route fraction L_T/L_{avail}	0.4%	1.1%	20%	25%	23%	18%
DD2 interconnections	*m1*	*m2*	*m3*	*m4*	*m5*	$m1-m5$
L_{avail} (m)	3.14	2.8	6.75	12.6	3.57	28.9
L_T (m)	0.0167	0.0364	1.40	3.30	0.657	5.4
needed route fraction L_T/L_{avail}	0.53%	1.3%	21%	26%	18%	19%

TABLE IX

DETAILED VIA CHARACTERISTICS OF INTERCONNECTIONS FOR ALL N UNIT-LEVEL SIGNALS IN THE DD1 IFU AND DD2 IFU. THE NUMBER OF VIAS PER LAYER AND TOTAL NUMBER OF VIAS ARE SHOWN.

DD1 interconnections	*v1*	*v2*	*v3*	*v4*	$v1 - v4$
v_T	6509	10349	29817	6887	53562
DD2 interconnections	*v1*	*v2*	*v3*	*v4*	$v1 - v4$
v_T	6030	9705	25522	6937	48194

TABLE X

OVERVIEW OF THE NUMBER OF VIAS v_T, TOTAL INTERCONNECT LENGTH L *(meters)*, NUMBER OF ELECTRICAL SHORTS s, AND NUMBER OF UNROUTED SIGNALS $N_{unroutes}$ IN THE DD1 IFU AND DD2 IFU ROUTED WITH DIFFERENT VALUES OF THE AUTOMATED ROUTER COST PARAMETERS $\{c_{v_j}\}$ ($j = 1$ THROUGH 4) FOR THE VIA LAYERS *v1,v2,v3,v4* AND COST PARAMETERS $\{c_{v_k}\}$ ($k = 1$ THROUGH 5) FOR THE METAL LAYERS *m1,m2,m3,m4,m5*. THE TABLE SHOWS THE VALUES OF THE COST PARAMETERS c_{m1} AND c_{m2} FOR ROUTES ON LOWER-LEVEL METAL AND THE COST PARAMETERS c_{m3}, c_{m4}, c_{m5} FOR REGULAR (*reg*) AND WRONG-WAY (*perp*) ROUTES ON UPPER-LEVEL METAL. THE NUMBERS SHOWN IN BOLDFACE INDICATE THE VALUES OBTAINED IN THE DD1 IFU AND DD2 IFU, RESPECTIVELY

.

i	$\{c_{v_j}\}$	c_{m1}, c_{m2}	$\{c_{m3}, c_{m4}, c_{m5}\}$	v_T	L (m)	s	$N_{unroutes}$
		reg, perp	*reg, perp*	*DD1, DD2*	*DD1, DD2*	*DD1, DD2*	*DD1, DD2*
a	1	$4, 4$	$2, 4$	**53562**, 54861	**5.506**, 5.434	**0**, 0	**0**, 0
b	4	$4, 4$	$2, 4$	47357, **48194**	5.505, **5.433**	0, **0**	4, **0**
c	8	$4, 4$	$2, 4$	44217, 45122	5.505, 5.434	64, 0	5, 0
d	16	$4, 4$	$2, 4$	40761, 41665	5.507, 5.431	235, 0	12, 7
e	32	$4, 4$	$2, 4$	35205, 35686	5.392, 5.311	347, 266	139, 155
c	8	$4, 4$	$2, 4$	44217, 45122	5.505, 5.434	64, 0	5, 0
f	8	$4, 4$	$1, 4$	43233, 45148	5.513, 5.451	0, 24	4, 0
g	8	$4, 4$	$2, 8$	44718, 45561	5.504, 5.433	0, 0	5, 0
h	8	$1, 1$	$1, 1$	33867, 35742	5.476, 5.410	0, 4	0, 0

TABLE XI

OVERVIEW OF THE RATIOS r_a AND r_c OF LENGTH TO VIAS (IN UNITS OF $\mu m/via$) INSTANTIATED BY THE AUTOMATIC ROUTER AND BY CUSTOM INTERCONNECTIONS, RESPECTIVELY, AS WELL AS THE FRACTION OF LOWER-LEVEL METAL $f_{12} = (m1 + m2)/(m1 + m2 + m3 + m4 + m5)$ AND FRACTION OF UPPER-LEVEL METAL $f_{345} = (m3 + m4 + m5)/(m1 + m2 + m3 + m4 + m5)$ IN THE DD1 IFU AND DD2 IFU UNIT-LEVEL INTERCONNECTIONS WITH DIFFERENT VALUES OF THE AUTOMATED ROUTER COST PARAMETERS $\{c_{v_j}\}$ ($j = 1$ THROUGH 4) FOR THE VIA LAYERS *v1,v2,v3,v4* AND COST PARAMETERS $\{c_{v_k}\}$ ($k = 1$ THROUGH 5) FOR THE METAL LAYERS *m1,m2,m3,m4,m5*. THE TABLE SHOWS THE VALUES OF THE COST PARAMETERS c_{m1} AND c_{m2} FOR ROUTES ON LOWER-LEVEL METAL AND THE COST PARAMETERS c_{m3}, c_{m4}, c_{m5} FOR REGULAR (*reg*) AND WRONG-WAY (*perp*) ROUTES ON UPPER-LEVEL METAL. THE NUMBERS SHOWN IN BOLDFACE INDICATE THE VALUES OBTAINED IN THE DD1 IFU AND DD2 IFU, RESPECTIVELY

.

i	$\{c_{v_j}\}$	c_{m1}, c_{m2}	$\{c_{m3}, c_{m4}, c_{m5}\}$	r_r $(\mu m/via)$	r_c $(\mu m/via)$	f_{12}	f_{345}
		reg, perp	*reg, perp*	*DD1, DD2*	*DD1, DD2*	*DD1, DD2*	*DD1, DD2*
a	1	4, 4	2, 4	**76.5**, 73.5	**255.3**, 248.8	**0.010**, 0.010	**0.99**, 0.99
b	4	4, 4	2, 4	88.5, **85.7**	255.3, **248.8**	0.010, **0.010**	0.99, **0.99**
c	8	4, 4	2, 4	96.2, 92.8	255.3, 248.8	0.011, 0.010	0.989, 0.99
d	16	4, 4	2, 4	106.3, 102.2	255.3, 248.8	0.013, 0.013	0.987, 0.987
e	32	4, 4	2, 4	123.7, 119.9	255.3, 248.8	0.014, 0.015	0.986, 0.985
c	8	4, 4	2, 4	96.2, 92.8	255.3, 248.8	0.011, 0.010	0.989, 0.99
f	8	4, 4	1, 4	99.1, 93.2	255.3, 248.8	0.0098, 0.008	0.9902, 0.992
g	8	4, 4	2, 8	94.8, 92.7	255.3, 248.8	0.011, 0.010	0.989, 0.99
h	8	1, 1	1, 1	133.3, 123.3	255.3, 248.8	0.13, 0.125	0.87, 0.875

TABLE XII

OVERVIEW OF STACKED VIAS IN DD1 IFU AND DD2 IFU SIGNAL INTERCONNECTIONS: SINGLE STACKED VIAS *SSV*, DOUBLE STACKED VIAS *DSV*, AND TRIPLE STACKED VIAS *TSV* AS A FUNCTION OF DIFFERENT VALUES OF THE AUTOMATED ROUTER COST PARAMETERS $\{c_{v_j}\}$ ($j = 1$ THROUGH 4) FOR THE VIA LAYERS *v1,v2,v3,v4* AND COST PARAMETERS $\{c_{v_k}\}$ ($k = 1$ THROUGH 5) FOR THE METAL LAYERS *m1,m2,m3,m4,m5*. THE TABLE SHOWS THE VALUES OF THE COST PARAMETERS c_{m1} AND c_{m2} FOR ROUTES ON LOWER-LEVEL METAL AND THE COST PARAMETERS c_{m3}, c_{m4}, c_{m5} FOR REGULAR (*reg*) AND WRONG-WAY (*perp*) ROUTES ON UPPER-LEVEL METAL. THE NUMBERS SHOWN IN BOLDFACE INDICATE THE VALUES OBTAINED IN THE DD1 IFU AND DD2 IFU, RESPECTIVELY

.

i	$\{c_{v_j}\}$	c_{m1}, c_{m2}	$\{c_{m3}, c_{m4}, c_{m5}\}$	*SSV*	*DSV*	*TSV*
		reg, perp	*reg, perp*	*DD1, DD2*	*DD1, DD2*	*DD1, DD2*
a	1	4, 4	2, 4	**4923**, 4777	**657**, 676	**12**, 9
b	4	4, 4	2, 4	4149, **4034**	418, **387**	1, **1**
c	8	4, 4	2, 4	3760, 3718	389, 364	3, 2
d	16	4, 4	2, 4	3069, 3125	322, 300	0, 2
e	32	4, 4	2, 4	2225, 2237	273, 265	0, 2
c	8	4, 4	2, 4	3760, 3718	389, 364	3, 2
f	8	4, 4	1, 4	3579, 3734	551, 532	1, 2
g	8	4, 4	2, 8	3273, 3252	421, 343	1, 3
h	8	1, 1	1, 1	1748, 1869	112, 116	0, 2

TABLE XIII

INTERCONNECT EFFECTIVENESS IN THE DD2 IFU. FOR NETLENGTHS L: $\epsilon_{L_c}^{(i)}$, $\epsilon_{L_o}^{(i)}$, $\epsilon_{L_r}^{(i)}$, $\epsilon_{L}^{(i)}$, WITH THE CORRESPONDING VALUES FOR $p_{L_t}^{(i-1)}$, $p_{L_o}^{(i-1)}$, $p_{L_r}^{(i-1)}$ AND $\Delta L_t^{(i-1)}$, $L_o^{(i-1)}$, AND $L_r^{(i-1)}$. $\Delta L_t^{(i-1)}$, $L_o^{(i-1)}$, AND $L_r^{(i-1)}$ ARE EXPRESSED IN UNITS OF *meters*. THE VALUES FOR THE EFFECTIVENESSES $\epsilon_{L_c}^{(i)}$, $\epsilon_{L_o}^{(i)}$, $\epsilon_{L_r}^{(i)}$ AND $\epsilon_{L}^{(i)}$ ARE GIVEN IN %. FOR VIAS v: $\epsilon_{v_c}^{(i)}$, $\epsilon_{v_o}^{(i)}$, $\epsilon_{v_r}^{(i)}$, AND $\epsilon_{v}^{(i)}$ WITH THE CORRESPONDING VALUES FOR $p_{v_t}^{(i-1)}$, $p_{v_o}^{(i-1)}$, $p_{v_r}^{(i-1)}$, AND $\Delta v_t^{(i-1)}$, $v_o^{(i-1)}$, AND $v_r^{(i-1)}$. THE VALUES FOR $\epsilon_{v_c}^{(i)}$, $\epsilon_{v_o}^{(i)}$, $\epsilon_{v_r}^{(i)}$, AND $\epsilon_{v}^{(i)}$ ARE GIVEN IN %.

L	*custom interconnections in* R_i			*other routes in* R_i			*rest of routes in* $\overline{R}_i$			*all routes*	
i	$\epsilon_{L_c}^{(i)}(\%)$	$p_{L_t}^{(i-1)}$	$\Delta L_t^{(i-1)}$	$\epsilon_{L_o}^{(i)}(\%)$	$p_{L_o}^{(i-1)}$	$L_o^{(i-1)}$	$\epsilon_{L_r}^{(i)}(\%)$	$p_{L_r}^{(i-1)}$	$L_r^{(i-1)}$	$\epsilon_{L}^{(i)}(\%)$	$L^{(i-$
1	11.0	0.23	1.25	−4.9	0.50	2.73	−0.14	0.28	1.51	0.066	5.5
2	−0.94	0.021	0.09	0.15	0.13	0.59	−0.044	0.85	3.70	−0.036	5.4
3	13.2	0.13	0.54	−1.7	0.0038	0.016	−0.093	0.87	3.73	1.7	5.5
4	3.7	0.037	0.14	−1.9	0.19	0.70	0.20	0.78	2.91	−0.052	5.4
5	3.5	0.025	0.09	−0.96	0.21	0.74	−0.064	0.77	2.78	−0.16	5.4
6	10.3	0.029	0.10	−0.56	0.20	0.69	0.14	0.78	2.74	0.30	5.4
V	*custom interconnections in* R_i			*other routes in* R_i			*rest of routes in* $\overline{R}_i$			*all routes*	
i	$\epsilon_{v_c}^{(i)}(\%)$	$p_{v_t}^{(i-1)})$	$\Delta v_t^{(i-1)}$	$\epsilon_{v_o}^{(i)}(\%)$	$p_{v_o}^{(i-1)})$	$v_o^{(i-1)}$	$\epsilon_{v_r}^{(i)}(\%)$	$p_{v_r}^{(i-1)})$	$v_r^{(i-1)}$	$\epsilon_{v}^{(i)}(\%)$	$v^{(i-$
1	66.2	0.12	7300	−8.8	0.47	28269	−2.0	0.41	25198	3.0	607
2	57.7	0.022	1228	0.23	0.21	11996	−0.20	0.77	43241	1.1	589
3	66.1	0.16	8830	20.4	0.45	250	2.2	0.84	46217	12.5	582
4	26.7	0.025	1148	1.2	0.10	4633	0.29	0.89	39637	1.1	513
5	73.8	0.064	2801	0.47	0.20	9018	−0.28	0.73	32280	4.6	509
6	39.5	0.018	732	0.60	0.19	7967	1.1	0.79	32647	1.7	489

TABLE XIV

INTERCONNECT EFFECTIVENESS IN THE DD2 IFU. THE *mean*, *standard error*, *p-value*, *lower confidence bound LCB*, AND *upper confidence bound UCB* ARE SHOWN FOR CUSTOM ROUTES, OTHER ROUTES, AND THE REST OF THE ROUTES. THE CONFIDENCE INTERVALS HAVE COVERAGE OF 95%; FOR μ_{L_c} AND μ_{v_c} ONLY THE LOWER 95% BOUND IS GIVEN. NOTE THAT THE DD2 RESULTS ARE UNIFORMLY CONSISTENT WITH DD1 RESULTS.

Netlengths	*mean(%)*	*standard error(%)*	*p-value*	$LCB(\%)$	UC
custom interconnections	$\tilde{\mu}_{L_c} = 10.3$	$\hat{\sigma}(\hat{\mu}_{L_c}) = 1.5$	$p\text{-}value(\mu_{L_c}) = 0.00051$	7.3	
other routes	$\tilde{\mu}_{L_o} = -2.9$	$\hat{\sigma}(\hat{\mu}_{L_o}) = 1.1$	$p\text{-}value(\mu_{L_o}) = 0.042$	-5.6	$-$
rest of routes	$\tilde{\mu}_{L_r} = 0.044$	$\hat{\sigma}(\hat{\mu}_{L_r}) = 0.05$	$p\text{-}value(\mu_{L_r}) = 0.41$	-0.17	0
Vias	*mean(%)*	*standard error(%)*	*p-value*	$LCB(\%)$	UC
custom interconnections	$\tilde{\mu}_{v_c} = 63.7$	$\hat{\sigma}(\hat{\mu}_{v_c}) = 4.5$	$p\text{-}value(\mu_{v_c}) = 0.000015$	54.7	
other routes	$\tilde{\mu}_{v_o} = -3.7$	$\hat{\sigma}(\hat{\mu}_{v_o}) = 2.4$	$p\text{-}value(\mu_{v_o}) = 0.195$	-9.9	
rest of routes	$\tilde{\mu}_{v_r} = 0.36$	$\hat{\sigma}(\hat{\mu}_{v_r}) = 0.57$	$p\text{-}value(\mu_{L_r}) = 0.55$	-1.1	

List of Figures

References

[1] M. T. Bohr, "Interconnect scaling - The real limiter to high performance ULSI," in *IEDM Tech. Dig.*, 1995, pp. 241-244.

[2] A. Deutsch, G. V. Kopcsay, C. W. Surovic, B. J. Rubin, L. M. Terman, R. P. Dunne, Jr., T. A. Gallo, R. H. Dennard, "Modeling and characteristics of long on-chip interconnections for high-performance microprocessors," *IBM J. Res. Dev.* vol. 39, pp. 547-567, Sept. 1995.

[3] ITRS Semiconductor Industry Association, The International Technology Roadmap for Semiconductors, 1999.

[4] R. W. Keyes, "Fundamental limits in digital information processing," *Proc. IEEE*, vol. 69, pp. 267-278, Feb. 1981.

[5] R. W. Keyes, "The wire-limited logic chip," *IEEE J. Solid-State Circuits*, vol. SC-17, pp. 1232-1233, Dec. 1982.

[6] R. W. Keyes, "The power of connections," *IEEE Circ. Dev. Mag.*, vol. 7, pp. 32-35, May 1991.

[7] J. D. Meindl, "Opportunities for gigascale integration," *Solid State Tech.*, pp. 85-89, Dec. 1987.

[8] G. A. Sai-Halasz, "Performance trends in high-end processors," *Proc. IEEE*, vol. 83, pp. 20-36, Jan. 1995.

[9] R. F. Service, "Can chip devices keep shrinking?" *Science*, vol. 274, pp. 1834-1836, Dec. 1996.

[10] P. Solomon, "A comparison of semiconductor devices for high-speed logic," *Proc. IEEE*, vol. 70, pp. 489-509, May 1982.

[11] P. M. Solomon, "The need for low resistance interconnects in future high-speed and high-frequency devices and systems," *Proc. SPIE*, vol. 947, pp. 104-123, Mar. 1988.

[12] A. K. Stamper, "Interconnection scaling 1 GHz and beyond," *IBM MicroNews*, vol. 4, pp. 1-12, 1998.

[13] H. B. Bakoglu and J. D. Meindl, "Optimal interconnection circuits for VLSI," in *ISSCC Dig. Tech. Papers*, 1984, pp. 164-165.

[14] H. B. Bakoglu and J. D. Meindl, "Optimal interconnection circuits for VLSI," *IEEE Trans. Electron Devices*, vol. ED-32, pp. 903-909, May 1985.

[15] W. E. Donath, "Placement and average interconnection lengths of computer logic," *IEEE Trans. Circuits Syst.*, vol. CAS-26, pp. 272-277, Apr. 1979.

[16] D. C. Edelstein, G. A. Sai-Halasz, Y.-J. Mii, "VLSI on-chip interconnection performance simulations and measurements," *IBM J. Res. Dev.* vol. 39, pp. 383-401, Jul. 1995.

[17] M. Feuer, "Connectivity of random logic," *IEEE Trans. Comput.*, vol. C-31, pp. 29-33, Jan. 1982.

[18] Y.-J. Mii, "Performance consideration for the scaling of submicron on-chip interconnections," *Proc. SPIE*, vol. 1805, pp. 332-336, Sept. 1992.

[19] J. Qian, S. Pullela, and L. Pillage, "Modeling the 'effective capacitance' for the RC interconnect of CMOS gates," *IEEE Trans. Computer-Aided Design*, vol. 13, pp.1526-1535, Dec. 1994.

[20] T. Sakurai, "Approximation of wiring delay in MOSFET LSI," *IEEE J. Solid-State Circuits*, vol. SC-18, pp. 418-426, Aug. 1983.

[21] M. Y. L. Wisniewski, E. Yashchin, R. L. Franch, D. Conrady, G. Fiorenza, I. C. Noyan, "The physical design of on-chip interconnections, Part I: Quantification of interconnect properties," to be published.

[22] Bernard Rosner, *Fundamentals of Biostatistics.* Boston, MA: Duxbury Press, 1986.

[23] G. E. P. Box, W. G. Hunter, and J. S. Hunter, *Statistics for Experimenters.* New York, NY: John Wiley and Sons, 1978.

[24] C.-C. Chang and J. Cong, "Pseudo pin assignment with crosstalk noise control," in *Proc. ISPD*, 2000, pp. 41-47.

[25] C. J. Anderson, J. Petrovick, J. M. Keaty, J. Warnock, G. Nussbaum, J. M. Tendler, C. Carter, S. Chu, J. Clabes, J. DiLullo, P. Dudley, P. Harvey, B. Krauter, J. LeBlanc, P.-F. Lu, B. McCredie, G. Plumb, P. J. Restle, S. Runyon, M. Scheuermann, S. Schmidt, J. Wagoner, R. Weiss, S. Weitzel, B. Zoric, "Physical design of a fourth-generation POWER GHz microprocessor," in *ISSCC Dig. Techn. Papers*, 2001, pp. 232-233.

[26] K. Diefendorff, "Power4 focuses on memory bandwidth," *Microprocessor Report*, vol. 13, pp. 1-8, Oct. 1999.

[27] IBM, NY. IBM Enterprise server pSeries 680. [Online] Available: http://www-1.ibm.com/servers/eserver/pseries/hardware/enterprise/

[28] J. D. Warnock, J. Keaty, J. Petrovick, J. Clabes, C. J. Kircher, B. Krauter, P. Restle, B. Zoric, C. J. Anderson, "The circuit and physical design of the POWER4 microprocessor," *IBM J. Res. Dev.*, vol. 46, Jan. 2002.